

# Strong correlation between bonding network and critical temperature in hydrogen-based superconductors

Francesco Belli,<sup>1,2</sup> J. Contreras-Garcia,<sup>3</sup> and Ion Errea<sup>1,2,4</sup>

<sup>1</sup>*Centro de Física de Materiales (CSIC-UPV/EHU), Manuel de Lardizabal Pasealekua 5, 20018 Donostia/San Sebastián, Spain*

<sup>2</sup>*Fisika Aplikatua 1 Saila, Gipuzkoako Ingeniaritza Eskola, University of the Basque Country (UPV/EHU), Europa Plaza 1, 20018 Donostia/San Sebastián, Spain*

<sup>3</sup>*Laboratoire de Chimie Théorique (LCT), Sorbonne Université CNRS, 75005 Paris (France)*

<sup>4</sup>*Donostia International Physics Center (DIPC), Manuel de Lardizabal Pasealekua 4, 20018 Donostia/San Sebastián, Spain*

Recent experimental discoveries show that hydrogen-rich compounds can reach room temperature superconductivity, at least at high pressures. Also that there exist metallic hydrogen-abundant systems with critical temperatures of few Kelvin, or even with no trace of superconductivity at all. By analyzing through first-principles calculations the structural and electronic properties of more than one hundred compounds predicted to be superconductors in the literature, we determine that the capacity of creating a bonding network of connected localized units is the key to enhance the critical temperature in hydrogen-based superconductors, explaining the large variety of critical temperatures of superconducting hydrogen-rich materials. We define a magnitude named as the *networking value*, which correlates well with the predicted critical temperature, much better than any other descriptor analyzed thus far. This magnitude can be easily calculated for any compound by analyzing isosurfaces of the electron localization function. By classifying the studied compounds according to their bonding nature, we observe that the *networking value* correlates with the critical temperature for all bonding types. Our analysis also highlights that systems with weakened covalent bonds are the most promising candidates for reaching high critical temperatures. The discovery of the positive correlation between superconductivity and the bonding network offers the possibility of screening easily hydrogen-based compounds and, at the same time, sets clear paths for chemically engineering better superconductors.

## INTRODUCTION

The field of hydrogen-based superconductivity has progressed enormously since 1968, when Ashcroft first proposed that pressurized hydrogen may become a high temperature superconductor [1]. While the first discovered superconductors were Th<sub>4</sub>H<sub>15</sub> [2] in 1970 and PdH [3] in 1972, with not very promising critical temperatures ( $T_c$ ) of 7.6 K and 5 K respectively, the more recent experimental discoveries at high pressures show that superconductivity on hydrogen-based compounds can span from a few Kelvin to room temperature. Few examples are the recently synthesized PrH<sub>9</sub> [4], where  $T_c = 7$  K at 125 GPa, AlH<sub>3</sub> where no superconductivity was observed above 4 K despite the predictions [5], and, on the other extreme, H<sub>3</sub>S [6], YH<sub>9</sub> [7, 8], YH<sub>6</sub> [9], and LaH<sub>10</sub> [10, 11] all reaching critical temperatures well above 200 K at megabar pressures. In addition, the recent observation of a  $T_c$  of 288 K at 267 GPa in a compound formed by sulfur, carbon, and hydrogen [12] confirms that hydrogen-based superconductors can be room-temperature superconductors. This observation finally dismisses the maximal limits for  $T_c$  initially suggested by Cohen and Anderson for electron-phonon driven superconductivity [13]. Hydrogen-based compounds are thus the best currently available candidates to reach ambient temperature and pressure superconductivity.

In order to discover new compounds with high  $T_c$  at low pressures, a simple physical-chemical understanding of the properties enhancing the critical temperatures in

hydrogen-based systems is necessary. In this regard, the hundreds of compounds predicted to be superconductors with first principles crystal structure prediction techniques constitute a rich working dataset to extract conclusions [14–16]. Among these predictions, the highest  $T_c$  values are 300 K for pure metallic hydrogen [17, 18] and 326 K for the YH<sub>10</sub> binary compound [19]. Attempts have been made to increase  $T_c$  further through ternary compounds, for instance with H<sub>3</sub>S<sub>1-x</sub>P<sub>x</sub> [20] and Li<sub>2</sub>MgH<sub>16</sub> [21]. Aiming at extracting useful information from this dataset, two main routes are being explored: on the one hand, machine learning methods [22–24] are starting to be employed to further increase the list of predicted systems, although the obtained new compounds so far do not beat the already known; on the other hand, additional efforts are being invested into classifying these superconductors using simple footprints based on structural, chemical, and electronic properties [15, 23, 25]. These studies suggest hydrogen rich systems with highly symmetrical structures and high density of states (DOS) at the Fermi level are the best candidates for high-temperature superconductivity.

Even if these properties are able to suggest good trends, they serve necessary but not sufficient conditions. This ultimately means there are not good optimizers thus far: improving these parameters will not necessarily lead to an improvement of the superconducting critical temperatures. In other words, even if the footprints for a good superconductor are somewhat clear, we cannot yet rely on simple variables to estimate the superconducting temperatures, clarify the reason for such a broad spectrum

of  $T_c$  values, and, ultimately, chemically engineer better superconductors.

In this work we investigate the chemical, structural, and electronic properties through *ab initio* methods based on density functional theory (DFT) for a set of 178 hydrogen-based superconductors previously predicted in the literature [14], including pure hydrogen and binary compounds. Our ultimate goal is to provide a simple understanding of the origin of the high  $T_c$  in these compounds. We focus mainly on the electronic and structural properties by means of chemical bonding descriptors, hydrogen-hydrogen distance, electronic charge, and density of states at the Fermi level. We review the impact on the predicted  $T_c$  of many of these descriptors, which have been already somewhat studied on a case to case basis in the literature but do not reveal conclusive. We identify that the electron pairing and delocalization play instead the final role. This takes us to propose a universal descriptor based on the identification of electronic delocalization networks, identified by means of the electron localization function (ELF) [26–30], which quantifies the network of the electronic bonding. We define a simple magnitude, the *networking value*, which is easily obtained from the calculation of ELF isosurfaces. Such quantity reveals useful to have a first estimate of the superconducting critical temperature without the need of performing electron-phonon coupling calculations. To the best of our knowledge, it is the first time that such a descriptor is proposed in the literature. We believe the analysis of the *networking value* is the first step for a high-throughput analysis of potential new high- $T_c$  systems. It also provides clear paths for chemically engineering better hydrogen-based superconductors, guiding the quest for high- $T_c$  compounds among the vast possibilities offered by ternary compounds.

## RESULTS

**Chemical composition and bonding categories.** In order to provide a comprehensive understanding of the different type of hydrogen-based compounds predicted to exist in the literature, it is convenient to categorize them in families according to the nature of the chemical bonding of the hydrogen atoms in the system. Our classification is guided by the study of the ELF [26–30] and the atomic charge distribution obtained through the Bader analysis [31–34] (see Methods for more details). The ultimate goal of this investigation is to better understand what kind of chemical interaction is the most beneficial for superconductivity among these compounds.

After a thorough analysis of the ELF in our test set, we identify six different families according to the nature of the chemical bonding, namely, *molecular* systems, *covalent* systems, systems driven by *weak covalent hydrogen-hydrogen interactions*, systems with *electride* behavior, *ionic* systems, and *isolated* systems. In each case, the

nature of the bonds is identified through the analysis of the ELF saddle points between different atoms. Since bonding properties are mainly local, each system can belong to more than just one family. However, in order to simplify the analysis, we focus on the most dominant feature for each compound. A representative for each family, together with the distribution of the families through the groups of the periodic table and the amount of hydrogen fraction in each case, is shown in Fig. 1. The hydrogen fraction ( $H_f$ ) takes the following form:

$$H_f = \frac{N_H}{N_H + N_X}, \quad (1)$$

where  $N_H$  and  $N_X$  are the number of hydrogen and non-hydrogen atoms in the primitive cell, respectively.

The *molecular* family describes all systems having at least one pair of hydrogen atoms forming a molecule. The latter can be identified through the ELF analysis by locating an isosurface surrounding an isolated molecule at very high values of ELF (see the magenta surface around the hydrogen molecules in TeH<sub>4</sub> in Fig. 1). A system is chosen to be molecular if an isolated pair of hydrogen atoms appears connected at a value of ELF higher than 0.85, i.e., if the minimum ELF value in between the hydrogen atoms is above 0.85. Systems with *molecular* behavior appear between groups 1 to 4 and 13 to 17. All of them have a value of  $H_f > 0.6$ , meaning that in the unit cells there are at least two hydrogen atoms per host. We note that *molecular* systems tend to have very high values of  $H_f$ , which reflects that in most cases several molecules exist per host atom. The highest critical temperatures for these *molecular* compounds have been predicted for ScH<sub>12</sub>(33) and TeH<sub>4</sub>(150), with  $T_c$  values around 150 K (the number in parenthesis after a given compound corresponds to the index given for each compound in Supplementary Data Tables I - III). The critical temperatures of the *molecular* compounds span from few Kelvin to these high values.

The *covalent* family is composed of systems where covalent bonds between hydrogen and the host atoms are dominant. Throughout our discussion we shall label the host atom as X, with X ≠ H. For H-X bonds, the covalent character can be identified by an elongation toward the host atom of the ELF isosurface surrounding the hydrogen (i.e. a polarized covalent bond). This is exemplified by the purple surfaces pointing from the H (small spheres) to the P atoms (big spheres) in PH<sub>2</sub> in Fig. 1. *Covalent* systems appear for groups 13 to 17, and are mostly related to the host atom's *p* type orbital character. Some of the highest critical temperature for these systems have been predicted for H<sub>3</sub>S(138) at 200 K, BH<sub>3</sub>(77) at 125 K, and H<sub>3</sub>Se(148) at 110 K.

The *weak covalent hydrogen-hydrogen interaction* family is dominated by compounds with predominant weak H-H covalent interactions. The difference with the molecular case is that hydrogen molecules or clusters appear elongated or quasi dissociated. This is illustrated with

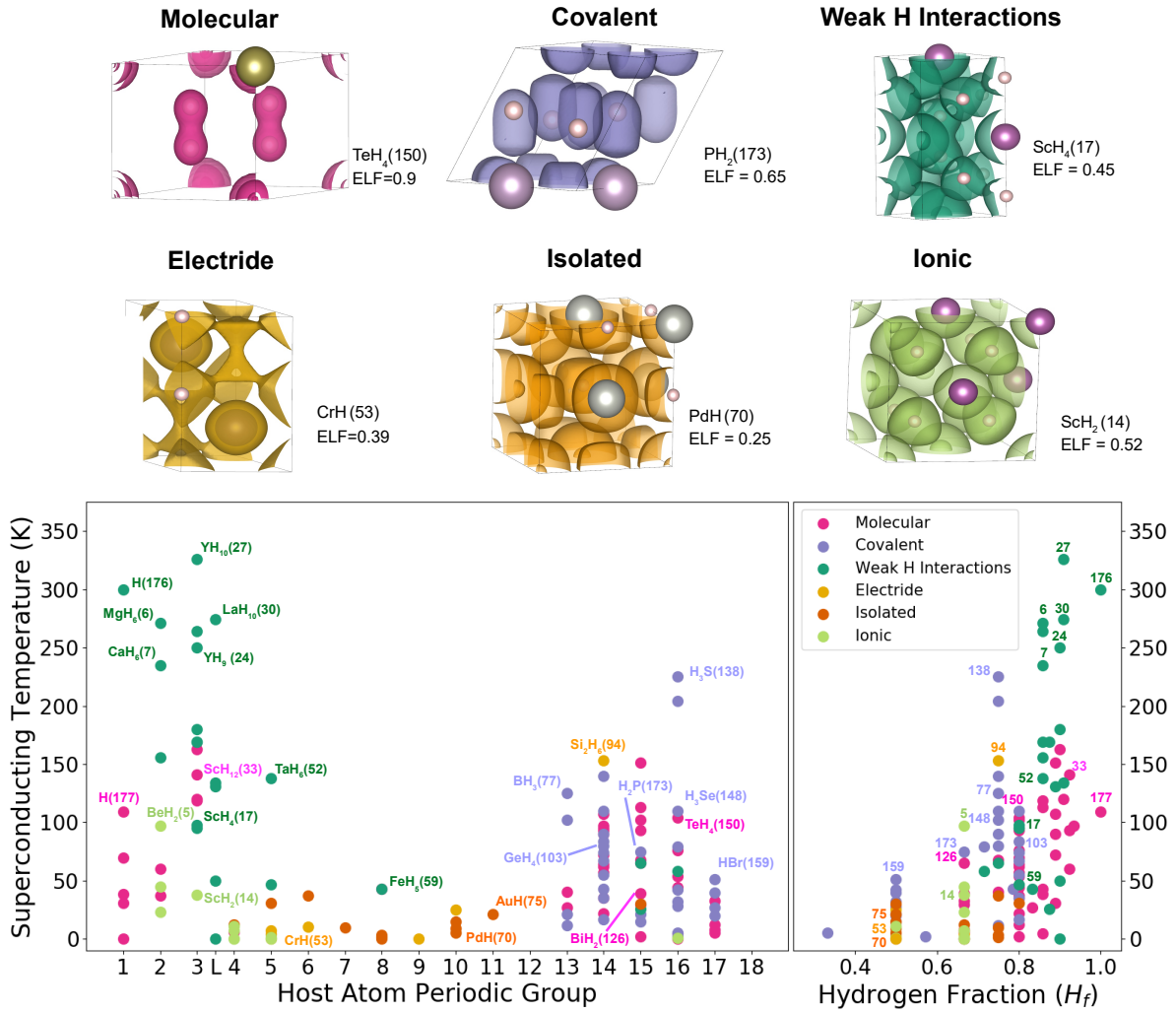


Figure 1. **Classification of hydrogen-based superconductors according to their bonding categories.** The top panel shows representative systems for the different categories with ELF isosurfaces at different values: TeH<sub>4</sub> for *molecular* systems (magenta), PH<sub>2</sub> for *covalent* systems (purple), ScH<sub>4</sub> for systems with *weak covalent hydrogen-hydrogen interactions* (dark green), CrH for *electrides* (yellow), PdH for *isolated* systems (orange), and ScH<sub>2</sub> for *ionic* systems (light green). The lower panel shows respectively the critical temperature as a function of the host atom periodic group (left panel) and the hydrogen fraction in the compounds (right panel). In the left panel, the name of some compounds is explicitly given together with the index (in parenthesis) given to each compound in Extended Data Tables I - III. In the right panel, and also in Figs. 2 and 4, just the index is given for these compounds for the sake of brevity.

the dark green surfaces in ScH<sub>4</sub> in Fig. 1, where bonds between hydrogen atoms appear at much lower values of ELF. From a quantitative point of view we assume that a group of hydrogen atoms is weakly bonded if the ELF at the bond point is within the range [0.4 - 0.85]. These systems mostly appear between groups 1 to 5. In this bonding type, interactions seem to be purely related to hydrogen atoms whilst the host atoms appear as inert or acting as a chemical pre-compressor or electron donor. Compounds with this bonding characteristic tend to contain many hydrogen atoms per host, as it happens for the molecular compounds. For compounds with the host atom in a low group of the periodic table, the host atoms

valence electrons are donated to the hydrogen atoms resulting in a weakening of the H-H bonds, which translates into an increment of the H-H distance. This family shows the highest predicted critical temperatures, the highest being 326 K for YH<sub>10</sub>(27) and 300 K for metallic hydrogen H(76).

The *ionic* family is formed by those systems whose hydrogen atoms show an ionic character. This is identified by an isolated proto-spherical ELF isosurfaces surrounding the hydrogen atoms. In addition, for a system to be hereby considered as *ionic* the mean extra charge per hydrogen atom must be more than 0.5 electrons. This is illustrated by the spherical light green surfaces around

hydrogen in  $\text{ScH}_2$  in Fig. 1, where the charge on H is 0.67 electrons. Ionic behavior was observed between groups 2 to 5 of the periodic table, in all cases with low values of  $H_f$ . The ionic bonding originates from the strong difference in electronegativity between host and hydrogen atoms, which is always increased under pressure [35]. This family transforms into the *weak covalent hydrogen-hydrogen interaction* class when  $H_f$  increases, since the donated charge becomes small in respect to the number of recipient hydrogen atoms. Critical temperatures for these systems are low, with the highest being 45 K for  $\text{BeH}_2$ (4).

The *electride* family contains systems featuring electride behavior, i.e. compounds with electrons localized in the voids. The latter can be identified by isolated pockets of localized electrons in empty space of the crystal as the ones shown in yellow for  $\text{CrH}$  in Fig. 1. From a quantitative viewpoint, electride behavior is characterized in terms of isolated isosurfaces not surrounding any nuclei with ELF maximum values in between 0.35 to 0.7. Note that metallic compounds are also included in this family. Metallic cases also show isolated bubbles of ELF occupying the voids, but their profile is flatter. Given the difficulties to set a quantitative barrier, we have merged them in a unique family. Electrides and metals only appear mainly between groups 5 and 10, and are among the systems with the lowest value of  $H_f$  reaching a maximum of 3 hydrogen atoms per host ( $H_f = 0.75$ ). Critical temperatures for these systems are low, not reaching above 50K, exception made for the  $\text{Si}_2\text{H}_6$ (94) with a  $T_c$  of 153 K, where the electride-metallic behavior seems to be arising from H-Si covalent bonds (not justifying a further differentiation between electrides and metals).

The remaining family includes all the materials featuring extremely weak bonds between hydrogen and host atoms. These systems have been named as *isolated* and are identified by the lack of any kind of connection of the ELF isosurfaces above 0.25. These systems have low critical temperatures not reaching above 40 K and appear mainly between groups 5 and 12 of the periodic table. They also show a weak capacity of hosting a large number of H atoms per X atom, as they have the lowest values of  $H_f$ .

Overall our results highlight that characterizing the bonding type of a solid thanks to these families enables to discard a great number of compounds as potential high- $T_c$  compounds. Covalent interactions, be it weak H-H or X-H are the most favorable for high-temperature superconductivity. This allows to identify the potential interesting combination of elements, especially with respect to the increasing search among ternary compounds. The lowest  $T_c$  values appear for *electrides* and *isolated* compounds, mostly appearing between groups 5 and 12, which do not show lots of potential as high- $T_c$  compounds. These families also show the lowest values of  $H_f$ .

**Hydrogen-hydrogen distance and electronic properties.** After categorizing the different bonding families of hydrogen-based superconductors, we focus on understanding the trends of the predicted  $T_c$  with structural and electronic properties. The results are summarized in Fig. 2. The analysis focuses on the shortest hydrogen-hydrogen distance for each compound, the charge distribution on hydrogen atoms, and the density of states at the Fermi level with the ultimate goal of finding correlations between such descriptors and the critical temperature.

Even if no general trend is observed when plotting  $T_c$  as a function of the H-H shortest distance, several conclusions can be drawn. The structural analysis highlights an increment of the superconducting critical temperature with the increase of the shortest hydrogen-hydrogen distance for those systems where the bonding is driven by pure hydrogen interactions, meaning the *molecular* and *weak covalent hydrogen-hydrogen interaction* families. For these two families the H-H distance spans from 0.74 Å for systems with  $T_c$  below 1 K to a maximum of around 1.35 Å for the compounds with highest critical temperatures. In the region between 0.9 and 1.35 Å lie the currently predicted compounds with the highest superconducting temperatures reaching values as high as 300 K. In other words, elongated H-H interactions promote  $T_c$ . Interestingly, our analysis highlights that such H-H distance variation is not related to a variation of pressure, meaning that on a broad level, increasing the pressure does not necessarily yield an increment of the bonding distance, so composition rather than pressure would be a more relevant variable to tweak (see Supplementary Data Table I to see the pressure at which each compound is studied).

The shortest hydrogen-hydrogen distance for the *covalent* family spans between 1 and 2.5 Å. Low symmetry *covalent* systems appear between 1 to 1.45 Å where the short H-H distance is due to inter hydrogen bonds appearing beside the dominant hydrogen-host bonds. The highest reported superconducting temperature for these systems is about 135 K for  $\text{BH}_3$ (77). Interestingly, at around 1.55 Å the *covalent* family shows a sharp spike in the predicted  $T_c$  through systems sharing linear  $X = H = X$  bonds originating through the host  $p$  orbitals, a  $\bar{3}m$  point group, a value of  $H_f$  equal to 0.75, and a lack of direct hydrogen-hydrogen bonds. Here lay systems as  $\text{H}_3\text{S}$ (138),  $\text{H}_3\text{Se}$ (148),  $\text{GaH}_3$ (80), and  $\text{GeH}_3$ (106). Interestingly, the  $\text{Si}_2\text{H}_6$ (94) *electride* also shares these features even if the bonding nature is slightly different. All these compounds are shown in Fig. 3 with a representative ELF isosurface. For H-H distances above approximately 1.55 Å a sharp drop in  $T_c$  appears, with systems not reaching above 50 K. This zone lacks direct hydrogen-hydrogen bonds and features systems with a low percentage of hydrogen, with mostly *isolated*, *electride*, and *ionic* behavior. Hence, covalent elongated bonds, H-H or H-X, with high  $H_f$  seem to be the best candidates to increase  $T_c$ .



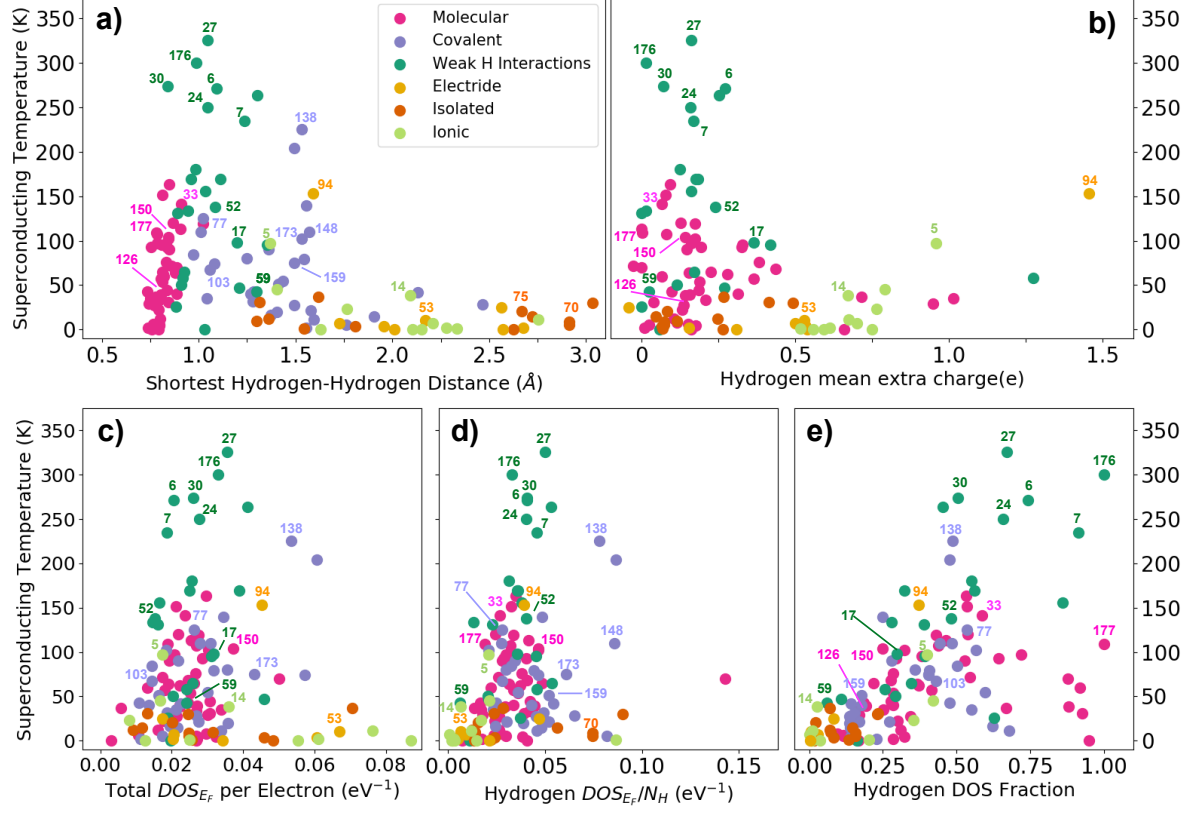


Figure 2. **Structural and electronic properties.** Panel **a)** shows  $T_c$  as a function of the shortest hydrogen-hydrogen distance for all the compounds. Panel **b)** shows  $T_c$  as a function of the mean extra electrons per hydrogen atom. Panels **c)**, **d)**, and **e)**, respectively, show  $T_c$  as a function of the total DOS at the Fermi level, the DOS at the Fermi level projected on the hydrogen  $s$  orbitals per hydrogen, and the fraction of the total DOS at the Fermi level coming from the hydrogen orbitals.

Panel **b** of Fig. 2 shows the mean extra electron per hydrogen atom obtained through the analysis of the Bader charge (see Methods). The *covalent* family has been excluded from this panel due to the unreliability of the Bader analysis, which arises from the difficulties in assigning shared electrons in the H-X bonds to each atom. We estimate the mean extra electron per hydrogen atom ( $\bar{\rho}$ ) as

$$\bar{\rho} = \frac{\sum_{i=1}^{N_H} Q_i - N_H}{N_H}, \quad (2)$$

where  $Q_i$  is the number of electrons assigned to the  $i$ th hydrogen atom by the Bader analysis, while  $N_H$  is the total number of hydrogen atoms in the primitive cell.

Overall hydrogen atoms tend to gain electrons due to their higher electronegativity with respect to other atoms in the cell. We observe that the highest  $T_c$  values are associated with small charge transfers, i.e. from 0 to 0.25 extra electrons per hydrogen atom. As the extra charge increases,  $T_c$  drops sharply below 50 K, exception made for the  $\text{BeH}_2$ (5), compound belonging to the *ionic* family with  $T_c = 97$  K, and  $\text{Si}_2\text{H}_6$ (94), with  $T_c = 153$  K and

part of the *electride* family.

It is often mentioned in the literature that an increment of (negative) charge on the hydrogen atom leads to a weakening of the hydrogen-hydrogen bonds [21, 36–38]. Our results show that both *molecular* and *weak covalent hydrogen-hydrogen interaction* families show non-negligible extra electrons on the hydrogen atoms. We also observe that the extra charge on the hydrogen is responsible for a slight increment of the H-H distance for the *weak covalent hydrogen-hydrogen interaction* family. In fact, compounds within this family with a shorter H-H distance tend to have less extra electrons per hydrogen atom. The maximum extra electron per hydrogen among this family is around 0.5, a value that increases up to 1 in the *molecular* systems.

Panels **c**, **d**, and **e** in Fig. 2 report the results for the DOS analysis. A simplified equation for the electron-phonon coupling constant ( $\lambda$ ) may be given by [39]

$$\lambda = \frac{N(E_F)\langle I^2 \rangle}{M\langle \omega^2 \rangle}, \quad (3)$$

where  $N(E_F)$  is the DOS at the Fermi energy,  $\langle I^2 \rangle$  is a

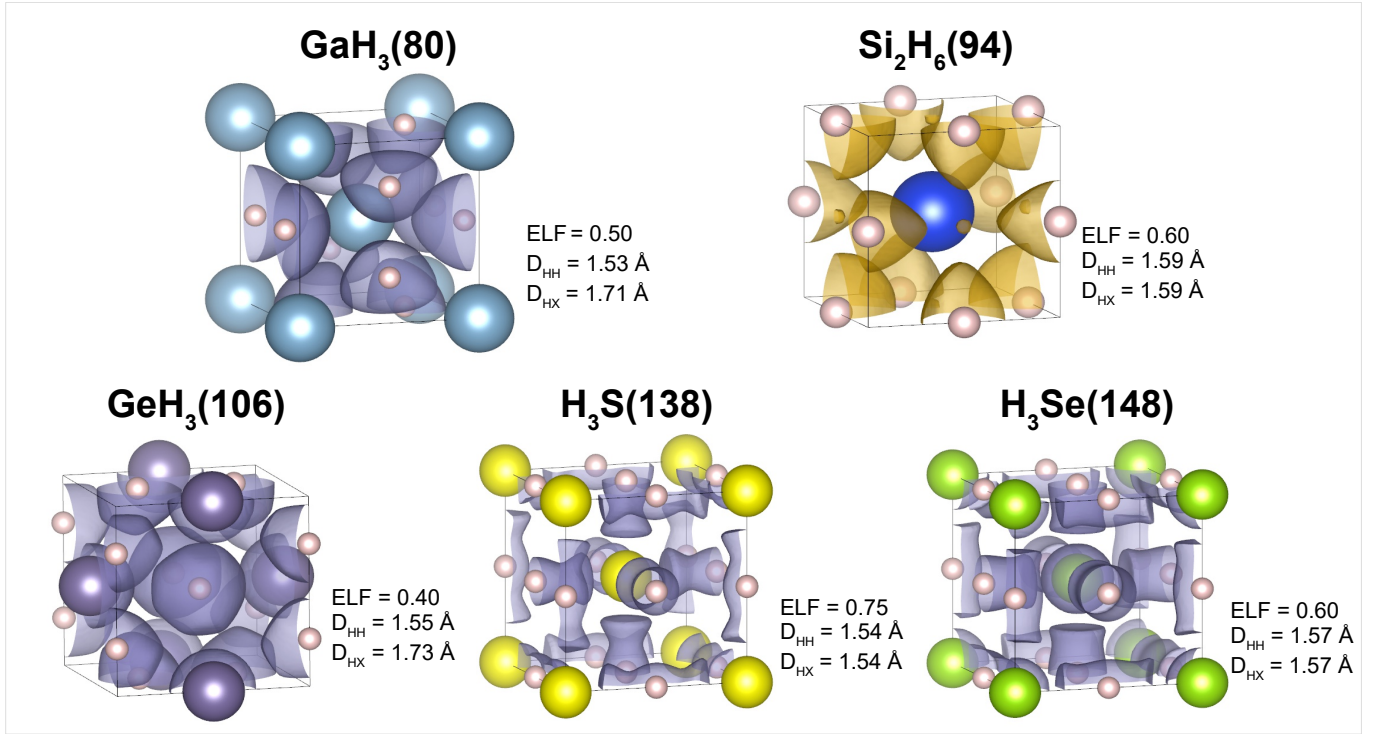


Figure 3. **Highly symmetric high- $T_c$  systems** . This figure shows five compounds related to the  $T_c$  spike around a hydrogen-hydrogen distance of 1.55 Å. The pink spheres refer to hydrogen atoms, while the rest refer to the respective host atoms. An ELF isosurface is depicted in each case. Also the shortest H-H ( $D_{HH}$ ) and H-X ( $D_{HX}$ ) distances are noted. Most of these compounds belong to the *covalent* family and show a purple ELF isosurface. The  $\text{Si}_2\text{H}_6$  compound is an *electride* (note the small ELF bubbles in empty sites) and its ELF isosurface is shown in orange.

term that is related to the electron-phonon matrix elements,  $M$  is the mean mass of the primitive cell, and  $\langle \omega^2 \rangle$  is the mean quadratic phonon frequency. This suggests that a higher  $N(E_F)$  should give rise to a higher electron-phonon coupling and, thus, also a higher superconducting critical temperature. Although this is a favorable condition for good superconductors, the results for the DOS prove this condition not to be univocally sufficient [40]. The total DOS per electron at the Fermi level shown in panel c of Fig. 2 shows a sharp increment in the highest superconducting temperatures for a DOS value of around  $0.015 \text{ eV}^{-1}$ . However, for such values of the DOS, compounds with very low  $T_c$  can still be found, making the total DOS at the Fermi level not a good descriptor of high- $T_c$  compounds.

Considering that H atoms due to their light mass are responsible for the large values of  $T_c$  in these compounds, we analyze the projection of the DOS at the Fermi level onto hydrogen atoms (see panel d of Fig. 2). However, the trends are similar to those obtained for the total DOS. In this case, the chance to have a higher superconducting critical temperature is related to an increment of DOS up to a value of  $0.06 \text{ eV}^{-1} N_H^{-1}$ . In particular, our results suggest that the key for high superconductivity is not strictly related to the value of the DOS. Instead, the

fraction of active hydrogen atoms at the Fermi energy (see panel e) seems to be more relevant. In agreement with our previous findings, only *molecular* and *weak covalent hydrogen-hydrogen interaction* families are able to reach high amounts of DOS coming from the hydrogen active atoms. This is directly related to the fact that the H-H bonds in those systems have a great contribution to the HOMO and LUMO. Nevertheless, false positives appear where the  $T_c$  appears very low despite the large contribution of hydrogen states to the Fermi surface. In fact, the DOS misses the information on how electrons are coupled with the lattice vibrations. Systems with very high values of the DOS at the Fermi energy but with very low electron-phonon coupling will not exhibit high superconducting critical temperatures.

**Networking through the ELF.** In order to screen new superconductors and guide the quest for new superconducting compounds, we need to look for an easily computable variable that will tell us not only about the interatomic bonding properties, but also how prone the system is to electron-phonon coupling. Even if some trends can be observed as discussed above, the descriptors analyzed so far in Figs. 1 and 2 are unable to capture when electrons couple more strongly to lattice vibrations and, thus, do not correlate with  $T_c$ . In this section we propose a new

observable based on the study of electron (de)localization that, instead, correlates well with the predicted superconducting critical temperature.

The ELF is a proper function to analyze the degree of electronic localization as high value isosurfaces of the ELF reveal regions in space where electrons localize. In fact, for isosurfaces with values close to 1 the electrons are localized generally on atomic sites, and they start to delocalize toward neighbors and form bonds as the ELF value decreases (see Methods). In order to analyze this delocalization on a crystal size scale, we define the *networking value*  $\phi$  as the highest value of the ELF that creates an isosurface spanning through the whole crystal in all three cartesian directions. The  $\phi$  value can thus be easily extracted by calculating the ELF and determining at which value a crystal sized isosurface is created when lowering the ELF value from 1. This isosurface encloses most of the atoms in the crystal, but not necessarily all. The ELF saddle points reveal crucial for the determination of the *networking value*, especially for hydrogen based compounds. For these systems, where hydrogen-hydrogen bonds are dominant, the ELF saddle points identify the interatomic bonds that pave the crystal sized network. Thus, for the determination of the *networking value* it is sufficient to identify the ensemble of ELF saddle points at the highest value of ELF able to bridge the gap between different atoms and create the 3D network.

In Fig. 4 we provide the ELF isosurface related to the  $\phi$  value as well as the network created by the saddle points for this ELF value for PdH(70), YH<sub>4</sub>(15), and H<sub>3</sub>S(138). These three cases are related to the most common types of networks identified during the analysis: *isolated*, *weak covalent hydrogen-hydrogen interaction*, and *covalent* families, respectively. In PdH(70) the network includes both Pd and H atoms. The isolated behavior of the atoms leads to the ELF bubbles around the atoms getting in contact at very low values of ELF, 0.19. For YH<sub>4</sub>(15) the highest 3D connecting network appears at ELF=0.43, and is constructed only by hydrogen atoms showing a weak covalent interaction. This is one of the cases in which the 3D network subsisting at the highest value of ELF does not include all the atoms in the unit cell. For the case of H<sub>3</sub>S(138), two interlaced networks appear at ELF=0.68 due to its high symmetry, which is supported by the weak  $H = S$  covalent bonds. Another type of network is the one arising from the *electride* systems, where the connection appears through the isolated pockets of charge in the empty zones of the unit cell.

Interestingly, the *networking value* correlates rather well with  $T_c$  as shown in Fig. 4, clearly much better than any other descriptor based on the structure or the electronic properties studied so far in the literature and in Figs. 1 and 2. We attribute this positive correlation to the capacity of this descriptor to somehow measure how the lattice vibrations affect the electronic cloud. This is not surprising, because if atoms are connected among

them with highly localized electrons, phonon vibrations are prone to affect more electrons. The fact that the network is required to span through all the crystal seems also reasonable, as all, or at least many, phonon modes are expected to affect the electronic cloud.

Few attempts were made to improve the correlation between  $\phi$  and  $T_c$  by introducing additional conditions for the network identification, such as having all the hydrogen atoms be part of the network, connecting the atoms through short direct paths, and creating connections between close hydrogen atoms up to a given distance. The introduction of these restrictions however produced only minor improvements at the prize of complicating the definition of  $\phi$ . On the opposite side, relaxing the condition about the 3D nature of the network to simply two dimensional sheets or one dimensional worms worsened the correlation. This suggests that forming a 3D bonding network is crucial, which we believe it is related to the fact that in this case the *networking value* better captures the overall coupling of the phonon modes with the electrons as argued above.

As seen in Fig. 4, an improvement in the correlation is obtained by multiplying  $\phi$  by the hydrogen fraction  $H_f$ :

$$\Phi = \phi H_f. \quad (4)$$

A reasonable explanation for such improvement is that the hydrogen fraction is a rough estimation of the multiplicity of hydrogen bonds. Systems with few H atoms will tend to form less bonds in which H atoms participate. This is in contrast with hydrogen rich systems with an incredible number of bonds in which H atoms participate. An example is HSe(148) with just 7 bonds per formula unit and  $H_f = 0.5$ , in contrast with LaH<sub>10</sub>(30) with 20 bonds per formula unit and  $H_f = 0.90$ .

We have also investigated the possible correlation between the *networking value* and the DOS which was found missing (see Fig. 5). The fact the *networking value* does not correlate at all with the DOS at the Fermi level, not even with the DOS coming from H atoms, underlines that these two descriptors are measuring different things. While  $\phi$  is able to capture the effect of the electron-phonon interaction, the DOS cannot, and consequently does not correlate well with  $T_c$ . On the contrary,  $\phi$ , or its product with the hydrogen fraction  $\Phi$ , determine for the first time a magnitude that shows a striking correlation with  $T_c$ , and constitutes a first positive and cheap identification of hydrogen-based superconductors.

## DISCUSSION

After the large analysis presented in this work, we can conclude that the highest critical temperatures are achieved in the *molecular*, *covalent* and *weak covalent hydrogen-hydrogen interaction* families. These three families are different expressions of covalent bonds, where

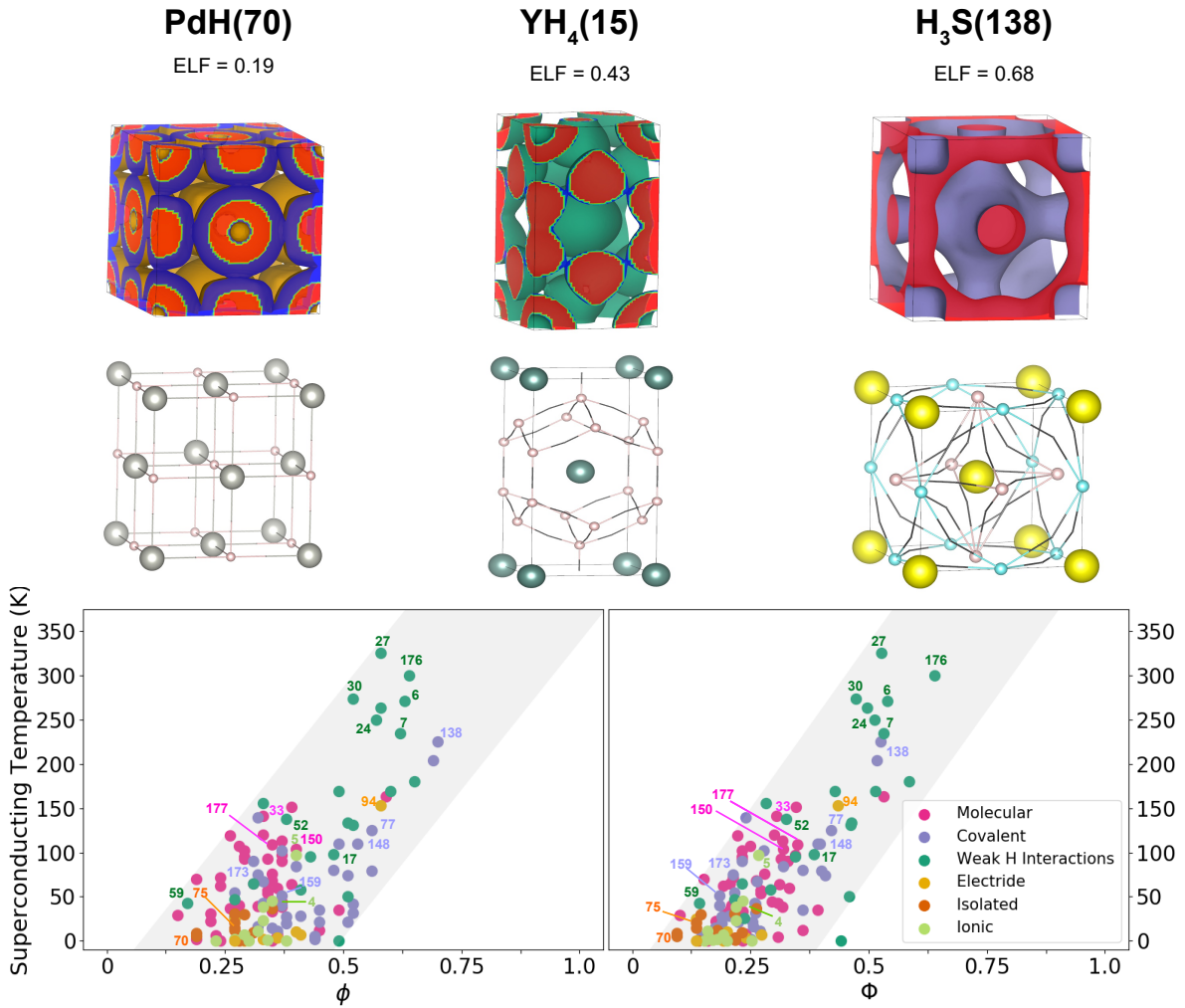


Figure 4. **Networking value.** The upper panel shows the ELF isosurface and the three dimensional network spanning through all the crystal, which is formed by the ELF saddle points and the atoms, associated with the  $\phi$  value for  $\text{PdH}(70)$ ,  $\text{YH}_4(15)$ , and  $\text{H}_3\text{S}(138)$ . The *networking value* is given for each case. The bottom panels show the critical temperature  $T_c$  as a function of the networking value  $\phi$  (left) and the networking value multiplied by  $H_f$ ,  $\Phi = \phi H_f$  (right). In both cases there is a linear correlation with the  $T_c$ , although  $\Phi$  correlates slightly better.

electrons are strongly localized. The highest critical temperatures appear between groups 1 and 5 of the periodic table, where bonds are mainly driven by covalent hydrogen-hydrogen interactions, and 13 and 16, where covalent bonds are predominantly between hydrogen and host atoms. It seems that these *covalent* compounds reach their highest  $T_c$  values for systems with large symmetry and hydrogen-host bonds at a distance of about 1.55 Å, without direct hydrogen-hydrogen bonding.

It is important to remark that our work shows how the *molecular* family transitions towards the *weak covalent hydrogen-hydrogen interaction* one, with an associated increase in  $T_c$ . The transition is smooth, starting from low  $T_c$  systems with only hydrogen molecules, such as  $\text{H}_4\text{I}(164)$ , going then through a mixed phase where molecules expand and intermolecular H-H interactions start to be present as for  $\text{ScH}_9(31)$  and  $\text{ScH}_7(34)$ , to fi-

nally transition towards a full weak interacting behavior with no molecules as found for  $\text{YH}_{10}(27)$  and  $\text{LaH}_{10}(30)$ , which have the largest *networking value* and  $T_c$ . This suggests that stretching hydrogen molecules is beneficial for superconductivity. The same conclusion is reached looking at the two pure hydrogen phases studied here (systems 176 and 177). The hydrogen phase ascribed to the *weak covalent hydrogen-hydrogen interaction* behavior (176) shows a far higher  $T_c$  of around 300 K compared to the purely molecular phase (177), with  $T_c = 109$  K. Therefore, stretching hydrogen molecules by chemical or mechanical means in systems containing many  $\text{H}_2$  units seems a very promising path to discovering new high- $T_c$  compounds. This seems to put in context the extraordinary prediction of a critical temperature of 473 K in  $\text{Li}_2\text{MgH}_{16}$  [21], where doping a molecular  $\text{MgH}_{16}$  compound with Li brakes the molecular units, transforming



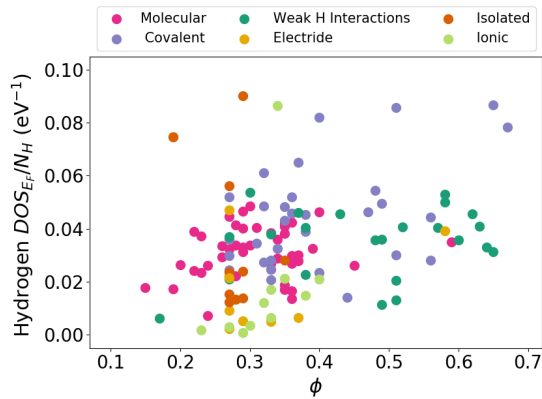


Figure 5. **Networking value with respect to the DOS.** The figure shows the *networking value*  $\phi$  as a function of the hydrogen contribution to the DOS at the Fermi energy per hydrogen atom.

the system into one with *weak covalent hydrogen-hydrogen interactions*.

The *networking value*  $\phi$  defined here is able to capture effectively how sensitive the electronic cloud is on average to lattice vibrations, and, consequently, correlates well with  $T_c$ . The *networking value* improves all other structural or electronic descriptors previously studied [15, 23, 25]. As extracting  $\phi$  simply requires the analysis of ELF isosurfaces, which can be easily obtained post-processing DFT ground state calculations, it offers a simple way of screening hydrogen-based superconductors, as well as showing the correct directions to chemically engineering better hydrogen-based superconductors. Interestingly, as the definition of  $\phi$  is completely general, not limited to the presence of hydrogen in the system, it could potentially be used to estimate the  $T_c$  of all phonon-mediated superconductors. Eventually, it may be also worth studying it in unconventional superconductors, as the  $\phi$  is only based on the analysis of the electronic cloud and correlations could also appear.

As a final word, we would like to underline that the superconducting critical temperatures used to find correlations are extracted directly from the literature, without being recalculated (see Supplementary Data Table I to check the reference from which the  $T_c$  value was taken for each case). All the  $T_c$  values were obtained by first principles DFT calculations, but at different levels of theory, for instance, for the estimation of the critical temperature. The wide grey area in Fig. 4 could be the result of such inconsistencies. In addition, most of these  $T_c$  values have been obtained assuming that the ground state structure is the one given by the minimum of the Born-Oppenheimer energy surface (classical approximation) and that lattice vibrations can be described within the harmonic approximation around these positions. However, in hydrogen-

based superconductors, recent calculations have shown that the crystal structure can be largely modified by ionic quantum effects and that anharmonicity strongly renormalizes the obtained harmonic phonon spectra, which can strongly impact the predicted  $T_c$  [18, 19, 41–47]. These effects could produce a narrower correlation between  $T_c$  and  $\phi$  by introducing variations due to corrections on the structure and  $T_c$ .

## METHODS

**DFT Calculations.** We carry out our analysis on a sample of 178 compounds containing hydrogen that had been previously predicted to be superconductors in the literature. Most of the chosen compounds were those summarized in Ref. [14], which had been analyzed before in the literature [36, 37, 48–136]. We took each of these compounds, relax them classically at a given pressure with DFT at the Born-Oppenheimer minimum position, and calculated electronic properties for them. Due to the immense work required, we did not perform the  $T_c$  calculations, but took the values predicted in the literature. Among the 178 compounds, 43 were discarded due to lack of information on the atomic structure, which made impossible their analysis. Supplementary Data Tables I-III summarize all the calculated data presented here, as well as from which reference the  $T_c$  value was taken.

All DFT calculations were performed with the plane-wave QUANTUM ESPRESSO (QE) package [137, 138]. The exchange correlation potential was approximated with the Perdew-Burke-Ernzerhof parametrization [139]. At least the first few upper core orbitals were included in the pseudopotential for the host atom. The cutoff for the wave-functions and the density were respectively 70 Ry and 700 Ry. Integrations over the Brillouin zone were performed with the Methfessel-Paxton smearing technique [140], with a 0.02 Ry broadening. These integrations were performed with dense  $\mathbf{k}$  point grids, where a volume of  $0.001 \text{ \AA}^{-3}$  was occupied per  $\mathbf{k}$  point in the Brillouin zone for the self-consistent calculation and a volume of  $0.0002 \text{ \AA}^{-3}$  for the non self-consistent calculation. The electronic properties such as the ELF, the DOS, and the charge distribution were calculated for each system using the QE post-processing tools through the results obtained for the non self-consistent calculations.

**Bader charges.** There have been numerous approaches in order to determine the charge associated to an atom in a molecule. Probably, one of the most useful in solid state is that derived from the electron density, introduced by Bader and coworkers in what is called the Quantum Theory of Atoms in Molecules [141]. In an ordinary solid, the electron density has its maxima (cusps) at the nuclei and decays exponentially as the electron density moves away from the nuclei. The resulting topology looks like an assemblage of mountains, each of which is identified as an

atom. The zero gradient surface around these maxima are well defined surfaces that lead to atoms as non-overlapping units. This allows determining their charge by mere integration of the electron density within their associated region of space. Since these regions are non-overlapping these charges have the advantageous properties of being additive.

**The Electron Localization Function.** The electron localization function (ELF) was developed by Becke and Edgecombe in 1990 [142] for the analysis in real space of electron localization, and later on reinterpreted by Savin [143] in terms of the Pauli kinetic energy density ( $t_p$ ) corrected by the homogeneous electron gas kinetic energy density ( $t_w$ ):

$$\chi = \frac{1}{1 + (t_p/t_w)^2}. \quad (5)$$

$\chi$  is then mapped to run from 0 to a maximum value of 1:

$$ELF = \frac{1}{1 + \chi^2}. \quad (6)$$

Values close to 1 appear in those places where electrons are localized. Hence, maxima appear in the bonds (as well as in cores and lone pairs). It should be noted that hydrogen constitutes a peculiar case. A molecule such as N<sub>2</sub> will feature a maximum in the middle of the inter-nitrogen distance associated with the N-N bond and separated from the N cores. Since a hydrogen molecule only has 2 electrons, a maximum does not appear for the H-H bond, but rather a surface with very high ELF that encapsulates the H<sub>2</sub> molecule.

It is easy to see from Eq. 6 that the value  $ELF = 0.5$  is associated with the distribution in a homogeneous electron gas of the same density as the point of study. Indeed, metals are characterized by very flat ELF profiles slightly deviating from 0.5.

Whereas the maxima of ELF provide a measure of how localized electrons are, its value in between these maxima characterize delocalization in between these regions, i.e. how easy it is for electrons to go from one localized unit to another [144]. When the “easiest pathway” is analyzed in the full crystalline cell, we end up with a picture of how easy it is for electrons to move across the crystal.

## DATA AVAILABILITY

All the results presented in this work are summarized in Supplementary Data Tables I-III. Further data or details are available from the corresponding author upon reasonable request.

## CODE AVAILABILITY

Quantum ESPRESSO is an open-source suite of computational tools available at [https://www.quantum-](https://www.quantum-espresso.org)

[espresso.org](https://www.quantum-espresso.org).

## REFERENCES

- [1] N. W. Ashcroft. Metallic hydrogen: A high-temperature superconductor? *Phys. Rev. Lett.*, 21:1748–1749, Dec 1968.
- [2] C. B. Satterthwaite and I. L. Toepke. Superconductivity of hydrides and deuterides of thorium. *Phys. Rev. Lett.*, 25:741–743, Sep 1970.
- [3] T. Skoskiewicz. Superconductivity in the palladium-hydrogen and palladium-nickel-hydrogen systems. *physica status solidi (a)*, 11(2):K123–K126, 1972.
- [4] Di Zhou, Dmitrii V. Semenov, Defang Duan, Hui Xie, Wuhao Chen, Xiaoli Huang, Xin Li, Bingbing Liu, Artem R. Oganov, and Tian Cui. Superconducting praseodymium superhydrides. *Science Advances*, 6(9), 2020.
- [5] Igor Goncharenko, M. I. Erements, M. Hanfland, J. S. Tse, M. Amboage, Y. Yao, and I. A. Trojan. Pressure-induced hydrogen-dominant metallic state in aluminum hydride. *Phys. Rev. Lett.*, 100:045504, Jan 2008.
- [6] A. P. Drozdov, M. I. Erements, I. A. Trojan, V. Ksenofontov, and S. I. Shylin. Conventional superconductivity at 203 kelvin at high pressures in the sulfur hydride system. *Nature*, 525:73, ags 2015.
- [7] PP Kong, VS Minkov, MA Kuzovnikov, SP Besedin, AP Drozdov, S Mozaffari, L Balicas, FF Balakirev, VB Prakapenka, E Greenberg, et al. Superconductivity up to 243 k in yttrium hydrides under high pressure. *arXiv preprint arXiv:1909.10482*, 2019.
- [8] Elliot Snider, Nathan Dasenbrock-Gammon, Raymond McBride, Xiaoyu Wang, Noah Meyers, Keith V. Lawler, Eva Zurek, Ashkan Salamat, and Ranga Dias. Superconductivity to 262 kelvin via catalyzed hydrogenation of yttrium at high pressures, 2020.
- [9] Ivan A. Trojan, Dmitrii V. Semenov, Alexander G. Kvashnin, Andrey V. Sadakov, Oleg A. Sobolevskiy, Vladimir M. Pudalov, Anna G. Ivanova, Vitali B. Prakapenka, Eran Greenberg, Alexander G. Gavriliuk, Viktor V. Struzhkin, Aitor Bergara, Ion Errea, Raffaello Bianco, Matteo Calandra, Francesco Mauri, Lorenzo Monacelli, Ryosuke Akashi, and Artem R. Oganov. Anomalous high-temperature superconductivity in yh<sub>6</sub>, 2020.
- [10] Maddury Somayazulu, Muhtar Ahart, Ajay K. Mishra, Zachary M. Geballe, Maria Baldini, Yue Meng, Viktor V. Struzhkin, and Russell J. Hemley. Evidence for superconductivity above 260 k in lanthanum superhydride at megabar pressures. *Phys. Rev. Lett.*, 122:027001, Jan 2019.
- [11] AP Drozdov, PP Kong, VS Minkov, SP Besedin, MA Kuzovnikov, S Mozaffari, L Balicas, FF Balakirev, DE Graf, VB Prakapenka, et al. Superconductivity at 250 k in lanthanum hydride under high pressures. *Nature*, 569(7757):528–531, 2019.
- [12] Elliot Snider, Nathan Dasenbrock-Gammon, Raymond McBride, Mathew Debessai, Hiranya Vindana, Kevin Vencatasamy, Keith V. Lawler, Ashkan Salamat, and Ranga P. Dias. Room-temperature superconductivity in a carbonaceous sulfur hydride. *Nature*, 586(7829):373–377, 2020.

- [13] Marvin L. Cohen and P. W. Anderson. Comments on the maximum superconducting transition temperature. *AIP Conference Proceedings*, 4(1):17–27, 1972.
- [14] Tiange Bi, Niloofer Zarifi, Tyson Terpstra, and Eva Zurek. The search for superconductivity in high pressure hydrides. In *Reference Module in Chemistry, Molecular Sciences and Chemical Engineering*. Elsevier, 2019.
- [15] Jos   A. Flores-Livas, Lilia Boeri, Antonio Sanna, Gianni Profeta, Ryotaro Arita, and Mikhail Erements. A perspective on conventional high-temperature superconductors at high pressure: Methods and materials. *Physics Reports*, 856:1 – 78, 2020. A perspective on conventional high-temperature superconductors at high pressure: Methods and materials.
- [16] Chris J. Pickard, Ion Errea, and Mikhail I. Erements. Superconducting hydrides under pressure. *Annual Review of Condensed Matter Physics*, 11(1):57–76, 2020.
- [17] Christoph Heil, Simone di Cataldo, Giovanni B. Bachelet, and Lilia Boeri. Superconductivity in sodalite-like yttrium hydride clathrates. *Phys. Rev. B*, 99:220502, Jun 2019.
- [18] Miguel Borinaga, Ion Errea, Matteo Calandra, Francesco Mauri, and Aitor Bergara. Anharmonic effects in atomic hydrogen: Superconductivity and lattice dynamical stability. *Phys. Rev. B*, 93:174308, May 2016.
- [19] Miguel Borinaga, P Riego, A Leonardo, Matteo Calandra, Francesco Mauri, Aitor Bergara, and Ion Errea. Anharmonic enhancement of superconductivity in metallic molecularCmca - 4 hydrogen at high pressure: a first-principles study. *Journal of Physics: Condensed Matter*, 28(49):494001, oct 2016.
- [20] Yanfeng Ge, Fan Zhang, and Yugui Yao. First-principles demonstration of superconductivity at 280 k in hydrogen sulfide with low phosphorus substitution. *Phys. Rev. B*, 93:224513, Jun 2016.
- [21] Ying Sun, Jian Lv, Yu Xie, Hanyu Liu, and Yanming Ma. Route to a superconducting phase above room temperature in electron-doped hydride compounds under high pressure. *Phys. Rev. Lett.*, 123:097001, Aug 2019.
- [22] Michael J. Hutcheon, Alice M. Shipley, and Richard J. Needs. Predicting novel superconducting hydrides using machine learning approaches. *Phys. Rev. B*, 101:144505, Apr 2020.
- [23] Takahiro Ishikawa, Takashi Miyake, and Katsuya Shimizu. Materials informatics based on evolutionary algorithms: Application to search for superconducting hydrogen compounds. *Phys. Rev. B*, 100:174506, Nov 2019.
- [24] Valentin Stanev, Corey Oses, A. Gilad Kusne, Efrain Rodriguez, Johnpierre Paglione, Stefano Curtarolo, and Ichiro Takeuchi. Machine learning modeling of superconducting critical temperature. *npj Computational Materials*, 4, June 2018.
- [25] Dmitrii V. Semenok, Ivan A. Kruglov, Igor A. Savkin, Alexander G. Kvashnin, and Artem R. Oganov. On distribution of superconductivity in metal hydrides. *Current Opinion in Solid State and Materials Science*, 24(2):100808, 2020.
- [26] A. D. Becke and K. E. Edgecombe. A simple measure of electron localization in atomic and molecular systems. *The Journal of Chemical Physics*, 92(9):5397–5403, 1990.
- [27] Andreas Savin, Ove Jepsen, J  rgen Flad, Ole Krogh Andersen, Heinzwerner Preuss, and Hans Georg von Schnering. Electron localization in solid-state structures of the elements: the diamond structure. *Angewandte Chemie International Edition in English*, 31(2):187–188, 1992.
- [28] Yuri Grin, Andreas Savin, and Bernard Silvi. *The ELF Perspective of chemical bonding*, chapter 10, pages 345–382. John Wiley and Sons, Ltd, 2014.
- [29] Patricio Fuentealba, E. Chamorro, and Juan C. Santos. Chapter 5 understanding and using the electron localization function. In Alejandro Toro-Labb  , editor, *Theoretical Aspects of Chemical Reactivity*, volume 19 of *Theoretical and Computational Chemistry*, pages 57 – 85. Elsevier, 2007.
- [30] Konstantinos Koumpouras and J Andreas Larsson. Distinguishing between chemical bonding and physical binding using electron localization function (ELF). *Journal of Physics: Condensed Matter*, 32(31):315502, may 2020.
- [31] W Tang, E Sanville, and G Henkelman. A grid-based bader analysis algorithm without lattice bias. *Journal of Physics: Condensed Matter*, 21(8):084204, jan 2009.
- [32] Edward Sanville, Steven D. Kenny, Roger Smith, and Graeme Henkelman. Improved grid-based algorithm for bader charge allocation. *Journal of Computational Chemistry*, 28(5):899–908, 2007.
- [33] Graeme Henkelman, Andri Arnaldsson, and Hannes Jonsson. A fast and robust algorithm for bader decomposition of charge density. *Computational Materials Science*, 36(3):354 – 360, 2006.
- [34] Min Yu and Dallas R. Trinkle. Accurate and efficient algorithm for bader charge integration. *The Journal of Chemical Physics*, 134(6):064111, 2011.
- [35] Martin Rahm, Roberto Cammi, NW Ashcroft, and Roald Hoffmann. Squeezing all elements in the periodic table: electron configuration and electronegativity of the atoms under compression. *Journal of the American Chemical Society*, 141(26):10253–10271, 2019.
- [36] Hui Wang, John S. Tse, Kaori Tanaka, Toshiaki Iitaka, and Yanming Ma. Superconductive sodalite-like clathrate calcium hydride at high pressures. *Proceedings of the National Academy of Sciences*, 109(17):6463–6466, 2012.
- [37] Feng Peng, Ying Sun, Chris J. Pickard, Richard J. Needs, Qiang Wu, and Yanming Ma. Hydrogen clathrate structures in rare earth hydrides at high pressures: Possible route to room-temperature superconductivity. *Phys. Rev. Lett.*, 119:107001, Sep 2017.
- [38] Hui Wang, Xue Li, Guoying Gao, Yinwei Li, and Yanming Ma. Hydrogen-rich superconductors at high pressures. *WIREs Computational Molecular Science*, 8(1):e1330, 2018.
- [39] W. L. McMillan. Transition temperature of strong-coupled superconductors. *Phys. Rev.*, 167:331–344, Mar 1968.
- [40] Lilia Boeri. *Understanding Novel Superconductors with Ab Initio Calculations*, pages 73–112. Springer International Publishing, Cham, 2020.
- [41] Ion Errea, Matteo Calandra, and Francesco Mauri. First-principles theory of anharmonicity and the inverse isotope effect in superconducting palladium-hydride compounds. *Phys. Rev. Lett.*, 111:177002, Oct 2013.
- [42] Ion Errea, Matteo Calandra, and Francesco Mauri. Anharmonic free energies and phonon dispersions from the stochastic self-consistent harmonic approximation: Application to platinum and palladium hydrides. *Phys. Rev. B*, 89:064302, Feb 2014.

- [43] Ion Errea, Francesco Belli, Lorenzo Monacelli, Antonio Sanna, Takashi Koretsune, Terumasa Tadano, Raffaello Bianco, Matteo Calandra, Ryotaro Arita, Francesco Mauri, and Jos   A. Flores-Livas. Quantum crystal structure in the 250-kelvin superconducting lanthanum hydride. *Nature*, 578:66 – 69, 2020.
- [44] Ion Errea, Matteo Calandra, and Francesco Mauri. First-principles theory of anharmonicity and the inverse isotope effect in superconducting palladium-hydride compounds. *Phys. Rev. Lett.*, 111:177002, Oct 2013.
- [45] Ion Errea, Matteo Calandra, Chris J. Pickard, Joseph R. Nelson, Richard J. Needs, Yinwei Li, Hanyu Liu, Yunwei Zhang, Yanming Ma, and Francesco Mauri. Quantum hydrogen-bond symmetrization in the superconducting hydrogen sulfide system. *Nature*, 532(7597):81–84, Apr 2016. Letter.
- [46] Raffaello Bianco, Ion Errea, Matteo Calandra, and Francesco Mauri. High-pressure phase diagram of hydrogen and deuterium sulfides from first principles: Structural and vibrational properties including quantum and anharmonic effects. *Physical Review B*, 97(21), June 2018.
- [47] Pugeng Hou, Francesco Belli, Raffaello Bianco, and Ion Errea. Strong anharmonic and quantum effects in pm-3n alh3 under high pressure: A first-principles study, 2021.
- [48] Tiange Bi, Niloofar Zarifi, Tyson Terpstra, and Eva Zurek. The search for superconductivity in high pressure hydrides. In *Reference Module in Chemistry, Molecular Sciences and Chemical Engineering*. Elsevier, 2019.
- [49] Yu Xie, Quan Li, Artem R. Oganov, and Hui Wang. Superconductivity of lithium-doped hydrogen under high pressure. *Acta Crystallographica Section C*, 70(2):104–111, Feb 2014.
- [50] Dawei Zhou, Xilian Jin, Xing Meng, Gang Bao, Yanming Ma, Bingbing Liu, and Tian Cui. Ab initio study revealing a layered structure in hydrogen-rich kh6 under high pressure. *Phys. Rev. B*, 86:014118, Jul 2012.
- [51] Shuyin Yu, Qingfeng Zeng, Artem R. Oganov, Chaohao Hu, Gilles Frapper, and Litong Zhang. Exploration of stable compounds, crystal structures, and superconductivity in the be-h system. *AIP Advances*, 4(10):107118, 2014.
- [52] Xiaolei Feng, Jurong Zhang, Guoying Gao, Hanyu Liu, and Hui Wang. Compressed sodalite-like mgh6 as a potential high-temperature superconductor. *RSC Adv.*, 5:59292–59296, 2015.
- [53] Yanchao Wang, Hui Wang, John S. Tse, Toshiaki Iitaka, and Yanming Ma. Structural morphologies of high-pressure polymorphs of strontium hydrides. *Phys. Chem. Chem. Phys.*, 17:19379–19385, 2015.
- [54] James Hooper, Bahadır Altintas, Andrew Shamp, and Eva Zurek. Polyhydrides of the alkaline earth metals: A look at the extremes under pressure. *The Journal of Physical Chemistry C*, 117(6):2982–2992, 2013.
- [55] Duck Young Kim, Ralph H. Scheicher, Ho-kwang Mao, Tae W. Kang, and Rajeev Ahuja. General trend for pressurized superconducting hydrogen-dense materials. *Proceedings of the National Academy of Sciences*, 107(7):2793–2796, 2010.
- [56] Yong-Kai Wei, Jiao-Nan Yuan, Faez Iqbal Khan, Guang-Fu Ji, Zhuo-Wei Gu, and Dong-Qing Wei. Pressure induced superconductivity and electronic structure properties of scandium hydrides using first principles calculations. *RSC Adv.*, 6:81534–81541, 2016.
- [57] Yinwei Li, Jian Hao, Hanyu Liu, S Tse John, Yanchao Wang, and Yanming Ma. Pressure-stabilized superconductive yttrium hydrides. *Scientific Reports*, 5:9948, 2015.
- [58] Shifeng Qian, Xiaowei Sheng, Xiaozhen Yan, Yangmei Chen, and Bo Song. Theoretical study of stability and superconductivity of sch<sub>n</sub> (n = 4 – 8) at high pressure. *Phys. Rev. B*, 96:094513, Sep 2017.
- [59] Xiaoqi Ye, Niloofar Zarifi, Eva Zurek, Roald Hoffmann, and NW Ashcroft. High hydrides of scandium under pressure: potential superconductors. *The Journal of Physical Chemistry C*, 122(11):6298–6309, 2018.
- [60] Bin Li, Zilong Miao, Lei Ti, Shengli Liu, Jie Chen, Zhixiang Shi, and Eugene Gregoryanz. Predicted high-temperature superconductivity in cerium hydrides at high pressures. *Journal of Applied Physics*, 126(23):235901, 2019.
- [61] Hanyu Liu, Ivan I. Naumov, Roald Hoffmann, N. W. Ashcroft, and Russell J. Hemley. Potential high-tc superconducting lanthanum and yttrium hydrides at high pressure. *Proceedings of the National Academy of Sciences*, 114(27):6990–6995, 2017.
- [62] IO Bashkin, MV Nefedova, VG Tissen, and EG Ponyatovskii. Superconductivity in the ti-d system under pressure. *Physics of the Solid State*, 40(12):1950–1952, 1998.
- [63] Kavungal Veedu Shanavas, L Lindsay, and David S Parker. Electronic structure and electron-phonon coupling in tih 2. *Scientific Reports*, 6:28102, 2016.
- [64] Xiao-Feng Li, Zi-Yu Hu, and Bing Huang. Phase diagram and superconductivity of compressed zirconium hydrides. *Phys. Chem. Chem. Phys.*, 19:3538–3543, 2017.
- [65] Yunxian Liu, Xiaoli Huang, Defang Duan, Fubo Tian, Hanyu Liu, Da Li, Zhonglong Zhao, Xiaojing Sha, Hongyu Yu, Huadi Zhang, et al. First-principles study on the structural and electronic properties of metallic hfh 2 under pressure. *Scientific reports*, 5:11381, 2015.
- [66] Changbo Chen, Fubo Tian, Defang Duan, Kuo Bao, Xilian Jin, Bingbing Liu, and Tian Cui. Pressure induced phase transition in mh2 (m = v, nb). *The Journal of Chemical Physics*, 140(11):114703, 2014.
- [67] Guoying Gao, Roald Hoffmann, N. W. Ashcroft, Hanyu Liu, Aitor Bergara, and Yanming Ma. Theoretical study of the ground-state structures and properties of niobium hydrides under pressure. *Phys. Rev. B*, 88:184104, Nov 2013.
- [68] Quan Zhuang, Xilian Jin, Tian Cui, Yanbin Ma, Qianqian Lv, Ying Li, Huadi Zhang, Xing Meng, and Kuo Bao. Pressure-stabilized superconductive ionic tantalum hydrides. *Inorganic chemistry*, 56(7):3901–3908, 2017.
- [69] Shuyin Yu, Xiaojing Jia, Gilles Frapper, Duan Li, Artem R Oganov, Qingfeng Zeng, and Litong Zhang. Pressure-driven formation and stabilization of superconductive chromium hydrides. *Scientific reports*, 5:17764, 2015.
- [70] Xiaofeng Li, Hanyu Liu, and Feng Peng. Crystal structures and superconductivity of technetium hydrides under pressure. *Phys. Chem. Chem. Phys.*, 18:28791–28796, 2016.
- [71] Alexander G Kvashnin, Ivan A Kruglov, Dmitrii V Semenok, and Artem R Oganov. Iron superhydrides feh5 and feh6: stability, electronic properties, and superconductivity. *The Journal of Physical Chemistry C*, 122(8):4731–4736, 2018.



- [72] Arnab Majumdar, John S. Tse, Min Wu, and Yansun Yao. Superconductivity in  $\text{FeH}_5$ . *Phys. Rev. B*, 96:201107, Nov 2017.
- [73] Yunxian Liu, Defang Duan, Fubo Tian, Chao Wang, Yanbin Ma, Da Li, Xiaoli Huang, Bingbing Liu, and Tian Cui. Stability and properties of the  $\text{ru-h}$  system at high pressure. *Phys. Chem. Chem. Phys.*, 18:1516–1520, 2016.
- [74] Yunxian Liu, Defang Duan, Xiaoli Huang, Fubo Tian, Da Li, Xiaojing Sha, Chao Wang, Huadi Zhang, Ting Yang, Bingbing Liu, et al. Structures and properties of osmium hydrides under pressure from first principle calculation. *The Journal of Physical Chemistry C*, 119(28):15905–15911, 2015.
- [75] Liyuan Wang, Defang Duan, Hongyu Yu, Hui Xie, Xiaoli Huang, Yanbin Ma, Fubo Tian, Da Li, Bingbing Liu, and Tian Cui. High-pressure formation of cobalt polychydrides: A first-principle study. *Inorganic Chemistry*, 57(1):181–186, 2018.
- [76] B Stritzker and W Buckel. Superconductivity in the palladium-hydrogen and the palladium-deuterium systems. *Zeitschrift für Physik A Hadrons and nuclei*, 257(1):1–8, 1972.
- [77] Ion Errea, Matteo Calandra, and Francesco Mauri. First-principles theory of anharmonicity and the inverse isotope effect in superconducting palladium-hydride compounds. *Physical review letters*, 111(17):177002, 2013.
- [78] Chao-Hao Hu, Artem R Oganov, Qiang Zhu, Guang-Rui Qian, Gilles Frapper, Andriy O Lyakhov, and Huai-Ying Zhou. Pressure-induced stabilization and insulator-superconductor transition of  $\text{bh}$ . *Physical review letters*, 110(16):165504, 2013.
- [79] Kazutaka Abe and NW Ashcroft. Crystalline diborane at high pressures. *Physical Review B*, 84(10):104118, 2011.
- [80] Yong-Kai Wei, Ni-Na Ge, Guang-Fu Ji, Xiang-Rong Chen, Ling-Cang Cai, Su-Qin Zhou, and Dong-Qing Wei. Elastic, superconducting, and thermodynamic properties of the cubic metallic phase of  $\text{alh}_3$  via first-principles calculations. *Journal of Applied Physics*, 114(11):114905, 2013.
- [81] Igor Goncharenko, MI Eremets, M Hanfland, JS Tse, M Amboage, Y Yao, and IA Trojan. Pressure-induced hydrogen-dominant metallic state in aluminum hydride. *Physical Review Letters*, 100(4):045504, 2008.
- [82] Pugeng Hou, Xiusong Zhao, Fubo Tian, Da Li, Defang Duan, Zhonglong Zhao, Binhua Chu, Bingbing Liu, and Tian Cui. High pressure structures and superconductivity of  $\text{alh}_3(\text{h}_2)$  predicted by first principles. *RSC Adv.*, 5:5096–5101, 2015.
- [83] Guoying Gao, Hui Wang, Aitor Bergara, Yinwei Li, Guangtao Liu, and Yanming Ma. Metallic and superconducting gallane under high pressure. *Physical Review B*, 84(6):064118, 2011.
- [84] Yunxian Liu, Defang Duan, Fubo Tian, Hanyu Liu, Chao Wang, Xiaoli Huang, Da Li, Yanbin Ma, Bingbing Liu, and Tian Cui. Pressure-induced structures and properties in indium hydrides. *Inorganic chemistry*, 54(20):9924–9928, 2015.
- [85] Y Yao, J. S Tse, Y Ma, and K Tanaka. Superconductivity in high-pressure  $\text{SiH}_4$ . *Europhysics Letters (EPL)*, 78(3):37003, apr 2007.
- [86] JS Tse, Y Yao, and K Tanaka. Novel superconductivity in metallic  $\text{snh}_4$  under high pressure. *Physical Review Letters*, 98(11):117004, 2007.
- [87] Ji Feng, Wojciech Grochala, Tomasz Jaroń, Roald Hoffmann, Aitor Bergara, and NW Ashcroft. Structures and potential superconductivity in  $\text{sih}_4$  at high pressure: En route to "metallic hydrogen". *Physical Review Letters*, 96(1):017006, 2006.
- [88] Huadi Zhang, Xilian Jin, Yunzhou Lv, Quan Zhuang, Yunxian Liu, Qianqian Lv, Kuo Bao, Da Li, Bingbing Liu, and Tian Cui. High-temperature superconductivity in compressed solid silane. *Scientific reports*, 5:8845, 2015.
- [89] Xiao-Jia Chen, Jiang-Long Wang, Viktor V Struzhkin, Ho-kwang Mao, Russell J Hemley, and Hai-Qing Lin. Superconducting behavior in compressed solid  $\text{sih}_4$  with a layered structure. *Physical review letters*, 101(7):077002, 2008.
- [90] Miguel Martinez-Canales, Artem R Oganov, Yanming Ma, Yan Yan, Andriy O Lyakhov, and Aitor Bergara. Novel structures and superconductivity of silane under pressure. *Physical review letters*, 102(8):087005, 2009.
- [91] Yinwei Li, Guoying Gao, Yu Xie, Yanming Ma, Tian Cui, and Guangtian Zou. Superconductivity at 100 k in dense  $\text{sih}_4(\text{h}_2)$  2 predicted by first principles. *Proceedings of the National Academy of Sciences*, 107(36):15708–15711, 2010.
- [92] Xilian Jin, Xing Meng, Zhi He, Yanming Ma, Bingbing Liu, Tian Cui, Guangtian Zou, and Ho-kwang Mao. Superconducting high-pressure phases of disilane. *Proceedings of the National Academy of Sciences*, 107(22):9969–9973, 2010.
- [93] Guoying Gao, Artem R Oganov, Aitor Bergara, Miguel Martinez-Canales, Tian Cui, Toshiaki Iitaka, Yanming Ma, and Guangtian Zou. Superconducting high pressure phase of germane. *Physical review letters*, 101(10):107002, 2008.
- [94] Chao Zhang, Xiao-Jia Chen, Yan-Ling Li, Viktor V Struzhkin, Russell J Hemley, Ho-Kwang Mao, Rui-Qin Zhang, and Hai-Qing Lin. Superconductivity in hydrogen-rich material:  $\text{Geh}_4$ . *Journal of superconductivity and novel magnetism*, 23(5):717–719, 2010.
- [95] Huadi Zhang, Xilian Jin, Yunzhou Lv, Quan Zhuang, Qianqian Lv, Yunxian Liu, Kuo Bao, Da Li, Bingbing Liu, and Tian Cui. Investigation of stable germane structures under high-pressure. *Physical Chemistry Chemical Physics*, 17(41):27630–27635, 2015.
- [96] Guohua Zhong, Chao Zhang, Xiaojia Chen, Yanling Li, Ruiqin Zhang, and Haiqing Lin. Structural, electronic, dynamical, and superconducting properties in dense  $\text{geh}_4(\text{h}_2)$  2. *The Journal of Physical Chemistry C*, 116(8):5225–5234, 2012.
- [97] PuGeng Hou, FuBo Tian, Da Li, ZhongLong Zhao, DeFang Duan, HuaDi Zhang, XiaoJing Sha, BingBing Liu, and Tian Cui. Ab initio study of germanium-hydride compounds under high pressure. *RSC advances*, 5(25):19432–19438, 2015.
- [98] M Mahdi Davari Esfahani, Artem R Oganov, Haiyang Niu, and Jin Zhang. Superconductivity and unexpected chemistry of germanium hydrides under pressure. *Physical Review B*, 95(13):134506, 2017.
- [99] Kazutaka Abe and NW Ashcroft. Quantum disproportionation: The high hydrides at elevated pressures. *Physical Review B*, 88(17):174110, 2013.
- [100] Huadi Zhang, Xilian Jin, Yunzhou Lv, Quan Zhuang, Yunxian Liu, Qianqian Lv, Da Li, Kuo Bao, Bingbing

- Liu, and Tian Cui. A novel stable hydrogen-rich snh 8 under high pressure. *RSC advances*, 5(130):107637–107641, 2015.
- [101] Guoying Gao, Artem R Oganov, Peifang Li, Zhenwei Li, Hui Wang, Tian Cui, Yanming Ma, Aitor Bergara, Andriy O Lyakhov, Toshiaki Iitaka, et al. High-pressure crystal structures and superconductivity of stannane (snh4). *Proceedings of the National Academy of Sciences*, 107(4):1317–1320, 2010.
- [102] JS Tse, Y Yao, and K Tanaka. Novel superconductivity in metallic snh 4 under high pressure. *Physical Review Letters*, 98(11):117004, 2007.
- [103] Huadi Zhang, Xilian Jin, Yunzhou Lv, Quan Zhuang, Ying Li, Kuo Bao, Da Li, Bingbing Liu, and Tian Cui. Pressure-induced phase transition of snh4: a new layered structure. *RSC Adv.*, 6:10456–10461, 2016.
- [104] M Mahdi Davari Esfahani, Zhenhai Wang, Artem R Oganov, Huafeng Dong, Qiang Zhu, Shengnan Wang, Maksim S Rakitin, and Xiang-Feng Zhou. Superconductivity of novel tin hydrides (sn n h m) under pressure. *Scientific reports*, 6:22873, 2016.
- [105] I. A. Troyan A.P. Drozdov, M. I. Erements. Superconductivity above 100 k in ph3 at high pressures. *arXiv:1508.06224*.
- [106] José A Flores-Livas, Maximilian Amsler, Christoph Heil, Antonio Sanna, Lilia Boeri, Gianni Profeta, Chris Wolverton, Stefan Goedecker, and ECU Gross. Superconductivity in metastable phases of phosphorus-hydride compounds under high pressure. *Physical Review B*, 93(2):020508, 2016.
- [107] Hanyu Liu, Yinwei Li, Guoying Gao, John S Tse, and Ivan I Naumov. Crystal structure and superconductivity of ph3 at high pressures. *The Journal of Physical Chemistry C*, 120(6):3458–3461, 2016.
- [108] Tiange Bi, Daniel P Miller, Andrew Shamp, and Eva Zurek. Superconducting phases of phosphorus hydride under pressure: stabilization by mobile molecular hydrogen. *Angewandte Chemie*, 129(34):10326–10329, 2017.
- [109] Tiange Bi, Daniel P Miller, Andrew Shamp, and Eva Zurek. Superconducting phases of phosphorus hydride under pressure: stabilization by mobile molecular hydrogen. *Angewandte Chemie*, 129(34):10326–10329, 2017.
- [110] Yuhao Fu, Xiangpo Du, Lijun Zhang, Feng Peng, Miao Zhang, Chris J Pickard, Richard J Needs, David J Singh, Weitao Zheng, and Yanming Ma. High-pressure phase stability and superconductivity of pnictogen hydrides and chemical trends for compressed hydrides. *Chemistry of Materials*, 28(6):1746–1755, 2016.
- [111] Kazutaka Abe and NW Ashcroft. Stabilization and highly metallic properties of heavy group-v hydrides at high pressures. *Physical Review B*, 92(22):224109, 2015.
- [112] Yanbin Ma, Defang Duan, Da Li, Yunxian Liu, Fubo Tian, Hongyu Yu, Chunhong Xu, Ziji Shao, Bingbing Liu, and Tian Cui. High-pressure structures and superconductivity of bismuth hydrides. *arXiv preprint arXiv:1511.05291*, 2015.
- [113] Yinwei Li, Jian Hao, Hanyu Liu, Yanling Li, and Yanming Ma. The metallization and superconductivity of dense hydrogen sulfide. *The Journal of chemical physics*, 140(17):174712, 2014.
- [114] Defang Duan, Yunxian Liu, Fubo Tian, Da Li, Xiaoli Huang, Zhonglong Zhao, Hongyu Yu, Bingbing Liu, Wenjing Tian, and Tian Cui. Pressure-induced metallization of dense (h 2 s) 2 h 2 with high-t c superconductivity. *Scientific reports*, 4:6968, 2014.
- [115] Ion Errea, Matteo Calandra, Chris J Pickard, Joseph R Nelson, Richard J Needs, Yinwei Li, Hanyu Liu, Yunwei Zhang, Yanming Ma, and Francesco Mauri. Quantum hydrogen-bond symmetrization in the superconducting hydrogen sulfide system. *Nature*, 532(7597):81–84, 2016.
- [116] Ryosuke Akashi, Mitsuki Kawamura, Shinji Tsuneyuki, Yusuke Nomura, and Ryotaro Arita. First-principles study of the pressure and crystal-structure dependences of the superconducting transition temperature in compressed sulfur hydrides. *Physical Review B*, 91(22):224513, 2015.
- [117] Yinwei Li, Lin Wang, Hanyu Liu, Yunwei Zhang, Jian Hao, Chris J Pickard, Joseph R Nelson, Richard J Needs, Wentao Li, Yanwei Huang, et al. Dissociation products and structures of solid h 2 s at strong compression. *Physical Review B*, 93(2):020103, 2016.
- [118] Takahiro Ishikawa, Akitaka Nakanishi, Katsuya Shimizu, Hiroshi Katayama-Yoshida, Tatsuki Oda, and Naoshi Suzuki. Superconducting h 5 s 2 phase in sulfur-hydrogen system under high-pressure. *Scientific reports*, 6:23160, 2016.
- [119] José A Flores-Livas, Antonio Sanna, and ECU Gross. High temperature superconductivity in sulfur and selenium hydrides at high pressure. *The European Physical Journal B*, 89(3):63, 2016.
- [120] Yanfeng Ge, Fan Zhang, and Yugui Yao. First-principles demonstration of superconductivity at 280 k in hydrogen sulfide with low phosphorus substitution. *Physical Review B*, 93(22):224513, 2016.
- [121] Shoutao Zhang, Yanchao Wang, Jurong Zhang, Hanyu Liu, Xin Zhong, Hai-Feng Song, Guochun Yang, Lijun Zhang, and Yanming Ma. Phase diagram and high-temperature superconductivity of compressed selenium hydrides. *Scientific reports*, 5(1):1–8, 2015.
- [122] Xin Zhong, Hui Wang, Jurong Zhang, Hanyu Liu, Shoutao Zhang, Hai-Feng Song, Guochun Yang, Lijun Zhang, and Yanming Ma. Tellurium hydrides at high pressures: High-temperature superconductors. *Physical Review Letters*, 116(5):057002, 2016.
- [123] Yunxian Liu, Defang Duan, Fubo Tian, Chao Wang, Gang Wu, Yanbin Ma, Hongyu Yu, Da Li, Bingbing Liu, and Tian Cui. Prediction of stoichiometric poh n compounds: crystal structures and properties. *RSC advances*, 5(125):103445–103450, 2015.
- [124] Defang Duan, Fubo Tian, Zhi He, Xing Meng, Liancheng Wang, Changbo Chen, Xiusong Zhao, Bingbing Liu, and Tian Cui. Hydrogen bond symmetrization and superconducting phase of hbr and hcl under high pressure: An ab initio study. *The Journal of chemical physics*, 133(7):074509, 2010.
- [125] Defang Duan, Fubo Tian, Zhi He, Xing Meng, Liancheng Wang, Changbo Chen, Xiusong Zhao, Bingbing Liu, and Tian Cui. Hydrogen bond symmetrization and superconducting phase of hbr and hcl under high pressure: An ab initio study. *The Journal of chemical physics*, 133(7):074509, 2010.
- [126] Siyu Lu, Min Wu, Hanyu Liu, S Tse John, and Bai Yang. Prediction of novel crystal structures and superconductivity of compressed hbr. *RSC Advances*, 5(57):45812–45816, 2015.
- [127] Changbo Chen, Ying Xu, Xiuping Sun, and Sihan Wang. Novel superconducting phases of hcl and hbr under high pressure: an ab initio study. *The Journal of Physical*

- Chemistry C*, 119(30):17039–17043, 2015.
- [128] Andrew Shamp and Eva Zurek. Superconducting high-pressure phases composed of hydrogen and iodine. *The Journal of Physical Chemistry Letters*, 6(20):4067–4072, 2015.
  - [129] Defang Duan, Fubo Tian, Yunxian Liu, Xiaoli Huang, Da Li, Hongyu Yu, Yanbin Ma, Bingbing Liu, and Tian Cui. Enhancement of  $T_c$  in the atomic phase of iodine-doped hydrogen at high pressures. *Physical Chemistry Chemical Physics*, 17(48):32335–32340, 2015.
  - [130] Xiaozhen Yan, Yangmei Chen, Xiaoyu Kuang, and Shikai Xiang. Structure, stability, and superconductivity of new  $\text{xe-h}$  compounds under high pressure. *The Journal of chemical physics*, 143(12):124310, 2015.
  - [131] David C Lonie, James Hooper, Bahadır Altıntaş, and Eva Zurek. Metallization of magnesium polyhydrides under pressure. *Physical Review B*, 87(5):054107, 2013.
  - [132] José A Flores-Livas, Maximilian Amsler, Christoph Heil, Antonio Sanna, Lilia Boeri, Gianni Profeta, Chris Wolverton, Stefan Goedecker, and EKH Gross. Superconductivity in metastable phases of phosphorus-hydride compounds under high pressure. *Physical Review B*, 93(2):020508, 2016.
  - [133] Andrew Shamp, Tyson Terpstra, Tiange Bi, Zackary Falls, Patrick Avery, and Eva Zurek. Decomposition products of phosphine under pressure:  $\text{Ph}_2$  stable and superconducting? *Journal of the American Chemical Society*, 138(6):1884–1892, 2016.
  - [134] Defang Duan, Fubo Tian, Xiaoli Huang, Da Li, Hongyu Yu, Yunxian Liu, Yanbin Ma, Bingbing Liu, and Tian Cui. Decomposition of solid hydrogen bromide at high pressure. *arXiv preprint arXiv:1504.01196*, 2015.
  - [135] Miguel Borinaga, Ion Errea, Matteo Calandra, Francesco Mauri, and Aitor Bergara. Anharmonic effects in atomic hydrogen: Superconductivity and lattice dynamical stability. *Physical Review B*, 93(17):174308, 2016.
  - [136] Miguel Borinaga, P Riego, A Leonardo, Matteo Calandra, Francesco Mauri, Aitor Bergara, and Ion Errea. Anharmonic enhancement of superconductivity in metallic molecular  $\text{cmca-4}$  hydrogen at high pressure: a first-principles study. *Journal of Physics: Condensed Matter*, 28(49):494001, 2016.
  - [137] Paolo Giannozzi, Stefano Baroni, Nicola Bonini, Matteo Calandra, Roberto Car, Carlo Cavazzoni, Davide Ceresoli, Guido L Chiarotti, Matteo Cococcioni, Ismaila Dabo, Andrea Dal Corso, Stefano de Gironcoli, Stefano Fabris, Guido Fratesi, Ralph Gebauer, Uwe Gerstmann, Christos Gougoussis, Anton Kokalj, Michele Lazzeri, Layla Martin-Samos, Nicola Marzari, Francesco Mauri, Riccardo Mazzarello, Stefano Paolini, Alfredo Pasquarello, Lorenzo Paulatto, Carlo Sbraccia, Sandro Scandolo, Gabriele Sclauzero, Ari P Seitsonen, Alexander Smogunov, Paolo Umari, and Renata M Wentzcovitch. QUANTUM ESPRESSO: a modular and open-source software project for quantum simulations of materials. *Journal of Physics: Condensed Matter*, 21(39):395502, sep 2009.
  - [138] P Giannozzi, O Andreussi, T Brumme, O Bunau, M Buongiorno Nardelli, M Calandra, R Car, C Cavazzoni, D Ceresoli, M Cococcioni, N Colonna, I Carnimeo, A Dal Corso, S de Gironcoli, P Delugas, R A DiStasio, A Ferretti, A Floris, G Fratesi, G Fugallo, R Gebauer, U Gerstmann, F Giustino, T Gorni, J Jia, M Kawamura, H-Y Ko, A Kokalj, E Küçükbenli, M Lazzeri, M Marsili, N Marzari, F Mauri, N L Nguyen, H-V Nguyen, A Otero de-la Roza, L Paulatto, S Poncé, D Rocca, R Sabatini, B Santra, M Schlipf, A P Seitsonen, A Smogunov, I Timrov, T Thonhauser, P Umari, N Vast, X Wu, and S Baroni. Advanced capabilities for materials modelling with quantum ESPRESSO. *Journal of Physics: Condensed Matter*, 29(46):465901, oct 2017.
  - [139] John P. Perdew, Kieron Burke, and Matthias Ernzerhof. Generalized Gradient Approximation Made Simple. *Phys. Rev. Lett.*, 77:3865–3868, Oct 1996.
  - [140] M. Methfessel and A. T. Paxton. High-precision sampling for brillouin-zone integration in metals. *Phys. Rev. B*, 40:3616–3621, Aug 1989.
  - [141] Bader R. F. W. Oxford University Press, Oxford, 1990.
  - [142] A.D. Becke and K.E. Edgecombe. *J. Chem. Phys.*, 92:5397, 1990.
  - [143] M. Kohout and A. Savin. *Int. J. Quant. Chem.*, 60:875, 1996.
  - [144] J. Contreras-Garcia and J. M. Recio. Electron delocalization and bond formation under the elf framework. *Theor. Chem. Acc.*, 128:411, 2011.

## ACKNOWLEDGEMENTS

This research was supported by the European Research Council (ERC) under the European Unions Horizon 2020 research and innovation programme (grant agreement No. 802533).

## AUTHOR CONTRIBUTIONS

F.B. performed all the DFT calculations. I.E. conceived the project. All authors contributed to the analysis of the data and to the writing of the manuscript.

## COMPETING INTERESTS

The authors declare no competing interests.

# Supplementary Information: Strong correlation between bonding network and critical temperature in hydrogen-based superconductors

Francesco Belli,<sup>1,2</sup> J. Contreras-Garcia,<sup>3</sup> and Ion Errea<sup>1,2,4</sup>

<sup>1</sup>*Centro de Física de Materiales (CSIC-UPV/EHU), Manuel de Lardizabal Pasealekua 5, 20018 Donostia/San Sebastián, Spain*

<sup>2</sup>*Fisika Aplikatua 1 Saila, Gipuzkoako Ingeniaritza Eskola, University of the Basque Country (UPV/EHU), Europa Plaza 1, 20018 Donostia/San Sebastián, Spain*

<sup>3</sup>*Laboratoire de Chimie Théorique (LCT), Sorbonne Université CNRS, 75005 Paris (France)*

<sup>4</sup>*Donostia International Physics Center (DIPC), Manuel de Lardizabal Pasealekua 4, 20018 Donostia/San Sebastián, Spain*

## CONTENTS

Supplementary Data Tables

1

References

10

## SUPPLEMENTARY DATA TABLES

**Supplementary Data Table I:** Table reporting item number used in the manuscript, chemical formula, space group, superconducting critical temperature as predicted, pressure at which it has been predicted, hydrogen fraction  $H_f$ , and the reference from which the  $T_c$  value has been extracted. The empty cells refer to missing values from the literature or to the impossibility to perform calculations.

Item	Chemical formula	Space group	$T_c$ (K)	Pressure (GPa)	$H_f$	Reference
0	LiH <sub>2</sub>	$P4/mbm$	0	150	0.666	[1]
1	LiH <sub>2</sub>	$R\bar{3}m$	38.34	140	0.857	[1]
2	LiH <sub>8</sub>	$I422$	31.04	200	0.888	[1]
3	KH <sub>6</sub>	$C2/c$	69.8	166	0.8	[2]
4	BeH <sub>2</sub>	$Cmcm$	45.1	204	0.666	[3]
5	BeH <sub>2</sub>	$P4/nmm$	97	349	0.666	[3]
6	MgH <sub>6</sub>	$Im\bar{3}m$	271	300	0.857	[4]
7	CaH <sub>6</sub>	$Im\bar{3}m$	235	150	0.857	[5]
8	SrH <sub>6</sub>	$R\bar{3}m$	156	250	0.857	[6]
9	BaH <sub>2</sub>	$R\bar{3}m$	0	60	-	[7]
10	BaH <sub>6</sub>	$P4/mmm$	38	70	-	[7]
11	ScH <sub>3</sub>	-	19.3	18	-	[8]
12	LaH <sub>3</sub>	$Cmcm$	22.5	11	-	[8]
13	YH <sub>3</sub>	-	40	17	-	[8]
14	ScH <sub>2</sub>	-	38.11	80	0.666	[9]
15	YH <sub>4</sub>	$I4/mmm$	95	120	0.8	[10]
16	YH <sub>6</sub>	$Im\bar{3}m$	264	120	0.857	[10]
17	ScH <sub>4</sub>	$I4/mmm$	98	200	0.8	[11]
18	ScH <sub>6</sub>	$Im\bar{3}m$	169	350	0.857	[12]
19	PrH <sub>9</sub>	$F\bar{4}3m$	0	100	0.9	[13]
20	CeH <sub>10</sub>	$Fm\bar{3}m$	134	200	0.909	[14]
21	CeH <sub>9</sub>	$P6_3/mmc$	50	100	0.9	[13]
22	LaH <sub>9</sub>	$Cc$	30	50	0.9	[13]
23	LaH <sub>6</sub>	$R\bar{3}c$	170	100	0.857	[13]
24	YH <sub>9</sub>	$P6_3/mmc$	250	150	0.9	[13]
25	ScH <sub>9</sub>	$P6_3/mmc$	180	400	0.9	[13]
27	YH <sub>10</sub>	$Fm\bar{3}m$	326	250	0.909	[13, 15]
28	LaH <sub>4</sub>	$I4/mmm$	10	300	0.8	[15]
29	LaH <sub>8</sub>	$C2/m$	131	300	0.888	[15]
30	LaH <sub>10</sub>	$Fm\bar{3}m$	274	150	0.909	[15]



31	ScH <sub>9</sub>	<i>I4<sub>1</sub>md</i>	163	300	0.9	[12]
32	ScH <sub>10</sub>	<i>Cmcm</i>	120	250	0.909	[12]
33	ScH <sub>12</sub>	<i>Immm</i>	141	350	0.923	[12]
34	ScH <sub>7</sub>	<i>Cmcm</i>	169	300	0.875	[12]
35	ScH <sub>3</sub>	<i>P6<sub>3</sub>/mmc</i>	1	400	-	[12]
36	ScH <sub>2</sub>	<i>P6/mmm</i>	4	300	-	[12]
37	ScH <sub>6</sub>	<i>P6<sub>3</sub>/mmc</i>	119	130	0.857	[12]
38	TiD <sub>0.74</sub>	—	4.43	30	-	[16]
39	TiH <sub>2</sub>	<i>Fm<math>\bar{3}</math>m</i>	7	0	0.666	[17]
40	TiH <sub>2</sub>	<i>I4/mmm</i>	0.002	0	0.666	[17]
41	ZrH	<i>Cmcm</i>	11	120	0.5	[18]
42	HfH <sub>2</sub>	<i>I4/mmm</i>	0	0	0.666	[19]
43	HfH <sub>2</sub>	<i>Cmma</i>	6	180	0.666	[19]
44	HfH <sub>2</sub>	<i>P2<sub>1</sub>/m</i>	12	260	0.666	[19]
45	NbH <sub>2</sub>	<i>P6<sub>3</sub>mc</i>	0.5	60	0.666	[20]
46	VH <sub>2</sub>	<i>Fm<math>\bar{3}</math>m</i>	0.5	0	0.666	[20]
47	NbH <sub>2</sub>	<i>Fm<math>\bar{3}</math>m</i>	1.5	0	0.666	[20]
48	NbH <sub>2</sub>	<i>Pnma</i>	4	60	0.666	[20]
49	NbH <sub>4</sub>	<i>I4/mmm</i>	47	300	0.8	[21]
50	TaH <sub>2</sub>	<i>Pnma</i>	7.1	200	0.666	[22]
51	TaH <sub>4</sub>	<i>R<math>\bar{3}</math>m</i>	31	250	0.8	[22]
52	TaH <sub>6</sub>	<i>Fdd2</i>	138.1	300	0.857	[22]
53	CrH	<i>P6<sub>3</sub>/mmc</i>	10.6	0	0.5	[23]
54	CrH <sub>3</sub>	<i>P6<sub>3</sub>/mmc</i>	37.1	81	0.75	[23]
55	TcH <sub>2</sub>	<i>I4/mmm</i>	10.64	200	0.666	[24]
56	TcH <sub>2</sub>	<i>Cmcm</i>	8.61	300	0.666	[24]
57	TcH <sub>3</sub>	<i>P4<sub>2</sub>/mmc</i>	9.94	300	0.75	[24]
58	FeH <sub>6</sub>	<i>Cmmm</i>	42.9	150	0.857	[25]
59	FeH <sub>5</sub>	<i>I4/mmm</i>	42.6	150	0.833	[25]
60	FeH <sub>5</sub>	<i>I4/mmm</i>	51	130	-	[26]
61	RuH	<i>Fm<math>\bar{3}</math>m</i>	0.41	100	0.5	[27]
62	RuH <sub>3</sub>	<i>Pm<math>\bar{3}</math>m</i>	3.57	125	0.75	[27]
63	RuH <sub>3</sub>	<i>Pm<math>\bar{3}</math>n</i>	1.25	200	0.75	[27]
64	OsH	<i>Fm<math>\bar{3}</math>m</i>	2.1	100	0.5	[28]
65	CoH	<i>Fm<math>\bar{3}</math>m</i>	0.11	5	0.5	[29]
66	R <sub>H</sub> H	<i>Fm<math>\bar{3}</math>m</i>	2.5	4	-	[30]
67	IrH	<i>Fm<math>\bar{3}</math>m</i>	7	8	-	[30]
68	PdH	—	9	0	0.5	[31]
69	PdD	—	11	0	-	[31]
70	PdH	<i>Fm<math>\bar{3}</math>m</i>	5	0	0.5	[32]
71	PdD	<i>Fm<math>\bar{3}</math>m</i>	6.5	0	-	[32]
72	PdT	<i>Fm<math>\bar{3}</math>m</i>	6.9	0	-	[32]
73	PtH	<i>Fm<math>\bar{3}</math>m</i>	15	100	0.5	[32]
74	PtH	<i>P6<sub>3</sub>/mmc</i>	25	80	0.5	[32]
75	AuH	<i>Fm<math>\bar{3}</math>m</i>	21	200	0.5	[30]
76	BH	<i>P6/mmm</i>	21.4	170	0.5	[33]
77	BH <sub>3</sub>	<i>Pbcn</i>	125	360	0.75	[34]
78	AlH <sub>3</sub>	<i>Pm<math>\bar{3}</math>n</i>	11.5	73	0.75	[35, 36]
79	AlH <sub>3</sub> (H <sub>2</sub> )	<i>P2<sub>1</sub>/m</i>	146	250	0.833	[37]
80	GaH <sub>3</sub>	<i>Pm<math>\bar{3}</math>n</i>	102	120	0.75	[38]
81	InH <sub>5</sub>	<i>P2<sub>1</sub>/m</i>	27.1	150	0.833	[39]
82	InH <sub>3</sub>	<i>R<math>\bar{3}</math></i>	40.5	200	0.75	[39]
83	SiH <sub>4</sub>	<i>C2/c</i>	55	125	0.8	[40]
84	SiH <sub>4</sub>	<i>P6/mmm</i>	74	120	0.8	[41]
85	SiH <sub>4</sub>	<i>Pmna</i>	166	202	-	[42]
86	SiH <sub>4</sub>	<i>C2/c</i>	30	300	-	[43]
87	SiH <sub>4</sub>	<i>P2<sub>1</sub>/c</i>	35	400	0.8	[43]
88	SiH <sub>4</sub>	<i>C2/m</i>	110	610	0.8	[43]
89	SiH <sub>4</sub>	<i>P<math>\bar{3}</math></i>	35.1	300	0.8	[43]
90	SiH <sub>4</sub>	<i>Cmca</i>	20	150	-	[44]
91	SiH <sub>4</sub>	<i>Pbcn</i>	16.5	190	0.8	[45]
92	SiH <sub>4</sub> H <sub>2</sub>	<i>Cmca</i>	107	250	-	[46]
93	Si <sub>2</sub> H <sub>6</sub>	<i>P<math>\bar{1}</math></i>	80	200	0.75	[47]
94	Si <sub>2</sub> H <sub>6</sub>	<i>Pm<math>\bar{3}</math>m</i>	153	275	0.75	[47]

95	Si <sub>2</sub> H <sub>6</sub>	<i>C2/c</i>	42	300	0.75	[47]
96	Si <sub>2</sub> H <sub>6</sub>	<i>Cmcm</i>	25	220	-	[47]
97	GeH <sub>4</sub>	<i>C2/c</i>	64	220	0.8	[48]
98	GeH <sub>4</sub>	<i>Cmmm</i>	47	20	-	[49]
99	GeH <sub>4</sub>	<i>Ama2</i>	57	250	0.8	[50]
100	GeH <sub>4</sub>	<i>C2/c</i>	84	500	0.8	[50]
101	GeH <sub>4</sub> (H <sub>2</sub> ) <sub>2</sub>	<i>P2<sub>1</sub>/c</i>	90	250	0.888	[51]
102	GeH <sub>3</sub>	<i>Cccm</i>	80	300	-	[52]
103	GeH <sub>4</sub>	<i>C2/m</i>	67	280	0.8	[53]
104	Ge <sub>3</sub> H <sub>11</sub>	<i>I4m2</i>	43	295	0.785	[53]
105	GeH <sub>3</sub>	<i>P4<sub>2</sub>/mmc</i>	90	180	0.75	[54]
106	GeH <sub>3</sub>	<i>Pm3m</i>	140	180	0.75	[54]
107	SnH <sub>8</sub>	<i>I4m2</i>	72	250	0.888	[55]
108	SnH <sub>4</sub>	<i>Ama2</i>	22	120	0.8	[56]
109	SnH <sub>4</sub>	<i>P6<sub>3</sub>/mmc</i>	62	200	0.8	[56]
110	SnH <sub>4</sub>	<i>P6/mmm</i>	80	120	-	[57]
111	SnH <sub>4</sub>	<i>C2/m</i>	95	600	0.8	[58]
112	SnH <sub>4</sub>	<i>I4/mmm</i>	92	220	-	[59]
113	SnH <sub>12</sub>	<i>C2/m</i>	93	250	0.923	[59]
114	SnH <sub>14</sub>	<i>C2/m</i>	97	300	0.933	[59]
115	PbH <sub>4</sub> (H <sub>2</sub> ) <sub>2</sub>	<i>C2/m</i>	107	130	0.888	[59]
116	PH <sub>3</sub>	-	100	226	-	[60]
117	PH	<i>I4/mmm</i>	81	230	-	[61]
118	PH <sub>2</sub>	<i>I4/mmm</i>	86	230	-	[61, 62]
119	PH <sub>4</sub>	<i>C2/m</i>	1.9	80	0.8	[63]
120	PH <sub>2</sub>	<i>Cmmm</i>	29.5	80	0.666	[64]
121	AsH	<i>Cmcm</i>	21.2	300	0.5	[65]
122	AsH <sub>8</sub>	<i>C2/c</i>	151.4	450	0.888	[65]
123	SbH	<i>Pnma</i>	14.6	175	0.5	[65]
124	SbH <sub>3</sub>	<i>Pmmn</i>	25.9	300	0.875	[65]
125	SbH <sub>4</sub>	<i>P6<sub>3</sub>/mmc</i>	102.2	150	0.8	[65]
126	BiH <sub>2</sub>	<i>Pnma</i>	39	125	0.666	[66]
127	BiH <sub>3</sub>	<i>I4<sub>1</sub>/amd</i>	65	270	0.75	[66]
128	SbH <sub>3</sub>	<i>Pnma</i>	68	170	0.75	[66]
129	BiH	<i>P6<sub>3</sub>/mmc</i>	30	250	0.5	[67]
130	BiH <sub>2</sub>	<i>P2<sub>1</sub>/m</i>	65	300	0.666	[67]
131	BiH <sub>4</sub>	<i>Pmmm</i>	93	150	0.8	[67]
132	BiH <sub>5</sub>	<i>C2/m</i>	119	300	-	[67]
133	BiH <sub>6</sub>	<i>P1</i>	113	300	0.857	[67]
134	H <sub>2</sub> S	<i>Cmca</i>	82	258	-	[68]
135	H <sub>2</sub> S	<i>P1</i>	60	258	-	[68]
136	(H <sub>2</sub> S) <sub>2</sub> H <sub>2</sub>	<i>Im3m</i>	204	200	0.75	[69]
137	(H <sub>2</sub> S) <sub>2</sub> H <sub>2</sub>	<i>R3m</i>	166	130	-	[69]
138	H <sub>3</sub> S	<i>Im3m</i>	225	150	0.75	[70]
139	H <sub>3</sub> S	<i>R3m</i>	214	170	-	[71]
140	H <sub>4</sub> S <sub>3</sub>	<i>Pnma</i>	2.1	140	0.571	[72]
141	H <sub>5</sub> S <sub>2</sub>	<i>P1</i>	79	130	0.714	[73]
142	D <sub>3</sub> S	<i>Im3m</i>	188	200	-	[74]
143	H <sub>3</sub> S <sub>0.925</sub> P <sub>0.075</sub>	<i>Im3m</i>	280	250	-	[75]
144	H <sub>3</sub> S <sub>0.9</sub> P <sub>0.1</sub>	<i>Im3m</i>	240	200	-	[75]
145	H <sub>3</sub> S <sub>0.96</sub> Si <sub>0.04</sub>	<i>Im3m</i>	275	250	-	[75]
146	HSe <sub>2</sub>	<i>C2/m</i>	5	300	0.333	[76]
147	HSe	<i>P4/nmm</i>	42	300	0.5	[76]
148	H <sub>3</sub> Se	<i>Im3m</i>	110	200	0.75	[76]
149	HSe	<i>P2<sub>1</sub>/c</i>	32	300	0.5	[76]
150	H <sub>4</sub> Te	<i>P6/mmm</i>	104	170	0.8	[77]
151	H <sub>5</sub> Te <sub>2</sub>	<i>C2/m</i>	58	200	0.714	[77]
152	HTe	<i>P4/nmm</i>	28	150	0.5	[77]
153	H <sub>4</sub> Te	<i>R3m</i>	76	270	0.8	[77]
154	HTe	<i>P6<sub>3</sub>/mmc</i>	44.2	300	0.8	[77]
155	PoH <sub>4</sub>	<i>C2/c</i>	53.6	250	0.8	[78]
156	PoH	<i>P6<sub>3</sub>/mmc</i>	0.65	300	0.5	[78]
157	PoH <sub>2</sub>	<i>Pnma</i>	0	200	0.666	[78]
158	PoH <sub>6</sub>	<i>C2/m</i>	4.68	200	0.857	[78]

159	HBr	$P2_1/m$	51	200	0.5	[79]
160	HCl	$P2_1/m$	40	360	0.5	[80]
161	HBr	$C2/m$	27	150	0.5	[81]
162	HCl	$C2/m$	20	250	0.5	[82]
163	H <sub>2</sub> I	$Cmcm$	8	100	0.666	[83]
164	H <sub>4</sub> I	$P6/mmm$	12.5	300	0.8	[84]
165	H <sub>2</sub> I	$Pnma$	5.3	100	0.666	[84]
166	H <sub>2</sub> I	$R\bar{3}m$	33	240	0.666	[84]
167	XeH	$Immm$	28	100	-	[85]
168	XeH <sub>2</sub>	$Cmcm$	26	400	-	[85]
169	MgH <sub>2</sub>	$P6_3/mmc$	23	180	0.666	[86]
170	MgH <sub>4</sub>	$Cmcm$	37	100	0.8	[86]
171	MgH <sub>12</sub>	$R\bar{3}$	60	140	0.923	[86]
172	PH <sub>3</sub>	$C2/m$	81	200	-	[87, 88]
173	PH <sub>2</sub>	$C2/m$	75	200	0.666	[87, 88]
174	H <sub>2</sub> Br	$Cmcm$	12.1	240	-	[89]
175	H <sub>4</sub> Br	$P6_3/mmc$	2.4	240	-	[89]
176	H	$I4_1/amd$	300	500	1	[90]
177	H	$Cmca\bar{4}$	109	450	1	[91]

**Supplementary Data Table II:** Table reporting the item index, chemical formula, *networking value*  $\phi$ , dominant bonding family assigned, and shortest H-H distance for all the compounds. The empty cells refer to missing values from the literature or to the impossibility to perform calculations.

Item	Chemical formula	<i>Networking value</i> $\phi$	Dominant bonding family	H-H Distance (Å)
0	LiH <sub>2</sub>	0.24	Molecular	0.759
1	LiH <sub>2</sub>	0.37	Molecular	0.803
2	LiH <sub>8</sub>	0.22	Molecular	0.844
3	KH <sub>6</sub>	0.19	Molecular	0.887
4	BeH <sub>2</sub>	0.35	Ionic	1.404
5	BeH <sub>2</sub>	0.4	Ionic	1.368
6	MgH <sub>6</sub>	0.63	Weak H Interactions	1.093
7	CaH <sub>6</sub>	0.62	Weak H Interactions	1.237
8	SrH <sub>6</sub>	0.33	Weak H Interactions	1.033
10	BaH <sub>6</sub>	-	-	-
9	BaH <sub>2</sub>	-	-	-
11	ScH <sub>3</sub>	-	-	-
12	LaH <sub>3</sub>	-	-	-
13	YH <sub>3</sub>	-	-	-
14	ScH <sub>2</sub>	0.33	Ionic	2.091
15	YH <sub>4</sub>	0.43	Weak H Interactions	1.352
16	YH <sub>6</sub>	0.58	Weak H Interactions	1.301
17	ScH <sub>4</sub>	0.48	Weak H Interactions	1.198
18	ScH <sub>6</sub>	0.6	Weak H Interactions	1.112
19	PrH <sub>9</sub>	0.49	Weak H Interactions	1.028
20	CeH <sub>10</sub>	0.51	Weak H Interactions	0.943
21	CeH <sub>9</sub>	0.51	Weak H Interactions	0.909
22	LaH <sub>9</sub>	0.13	Molecular	0.550
23	LaH <sub>6</sub>	-	-	0.944
24	YH <sub>9</sub>	0.57	Weak H Interactions	1.045
25	ScH <sub>9</sub>	0.65	Weak H Interactions	0.983
27	YH <sub>10</sub>	0.58	Weak H Interactions	1.047
28	LaH <sub>4</sub>	-	-	1.189
29	LaH <sub>8</sub>	0.52	Weak H Interactions	0.890
30	LaH <sub>10</sub>	0.52	Weak H Interactions	0.840
31	ScH <sub>9</sub>	0.59	Molecular	0.848
32	ScH <sub>10</sub>	0.33	Molecular	0.866
33	ScH <sub>12</sub>	0.33	Molecular	0.909
34	ScH <sub>7</sub>	0.49	Molecular	0.960
35	ScH <sub>3</sub>	-	-	-
36	ScH <sub>2</sub>	-	-	-
37	ScH <sub>6</sub>	0.26	Molecular	1.022
38	TiD <sub>0.74</sub>	-	-	-
39	TiH <sub>2</sub>	0.29	Ionic	2.210
40	TiH <sub>2</sub>	0.38	Ionic	1.628
41	ZrH	0.32	Ionic	2.753
42	HfH <sub>2</sub>	0.23	Ionic	2.149
43	HfH <sub>2</sub>	0.23	Molecular	0.765
44	HfH <sub>2</sub>	0.27	Isolated	1.359
45	NbH <sub>2</sub>	0.29	Electride	2.009
46	VH <sub>2</sub>	0.3	Ionic	2.105
47	NbH <sub>2</sub>	0.27	Ionic	2.277
48	NbH <sub>2</sub>	0.36	Electride	1.955
49	NbH <sub>4</sub>	0.27	Weak H Interactions	1.209
50	TaH <sub>2</sub>	0.41	Electride	1.728
51	TaH <sub>4</sub>	0.27	Isolated	1.313
52	TaH <sub>6</sub>	0.38	Weak H Interactions	1.085
53	CrH	0.4	Electride	2.171
54	CrH <sub>3</sub>	0.35	Isolated	1.615
55	TcH <sub>2</sub>	-	-	1.700
56	TcH <sub>2</sub>	-	-	1.241
57	TcH <sub>3</sub>	0.31	Isolated	1.299



58	FeH <sub>6</sub>	0.36	Molecular	0.733
59	FeH <sub>5</sub>	0.17	Weak H Interactions	1.300
60	FeH <sub>5</sub>	-	-	-
61	RuH	0.28	Isolated	2.626
62	RuH <sub>3</sub>	0.29	Isolated	1.807
63	RuH <sub>3</sub>	0.29	Isolated	1.542
64	OsH	0.33	Ionic	2.676
65	CoH	0.27	Metallic	2.570
66	R <sub>H</sub> H	-	-	-
67	IrH	-	-	-
68	PdH	0.19	Isolated	2.911
69	PdD	-	-	-
70	PdH	0.19	Isolated	2.911
71	PdD	-	-	-
72	PdT	-	-	-
73	PtH	0.27	Isolated	2.723
74	PtH	0.27	Ionic	2.563
75	AuH	0.27	Isolated	2.667
76	BH	0.51	Covalent	10000
77	BH <sub>3</sub>	0.56	Covalent	1.024
78	AlH <sub>3</sub>	0.36	Covalent	1.593
79	AlH <sub>3</sub> (H <sub>2</sub> )	-	-	0.842
80	GaH <sub>3</sub>	0.37	Covalent	1.531
81	InH <sub>5</sub>	0.27	Molecular	0.770
82	InH <sub>3</sub>	0.28	Molecular	0.884
83	SiH <sub>4</sub>	0.27	Covalent	1.435
84	SiH <sub>4</sub>	0.51	Covalent	1.081
85	SiH <sub>4</sub>	-	-	-
86	SiH <sub>4</sub>	-	-	-
87	SiH <sub>4</sub>	0.45	Covalent	1.043
88	SiH <sub>4</sub>	0.49	Covalent	1.009
89	SiH <sub>4</sub>	0.49	Molecular	0.750
90	SiH <sub>4</sub>	-	-	-
91	SiH <sub>4</sub>	0.32	Covalent	1.372
92	SiH <sub>4</sub> H <sub>2</sub>	-	-	-
93	Si <sub>2</sub> H <sub>6</sub>	0.48	Covalent	1.247
94	Si <sub>2</sub> H <sub>6</sub>	0.58	Electride	1.592
95	Si <sub>2</sub> H <sub>6</sub>	0.48	Molecular	0.592
96	Si <sub>2</sub> H <sub>6</sub>	-	-	-
97	GeH <sub>4</sub>	0.39	Molecular	0.878
98	GeH <sub>4</sub>	-	-	-
99	GeH <sub>4</sub>	0.34	Molecular	0.803
100	GeH <sub>4</sub>	0.4	Covalent	0.973
101	GeH <sub>4</sub> (H <sub>2</sub> ) <sub>2</sub>	0.37	Molecular	0.845
102	GeH <sub>3</sub>	-	-	-
103	GeH <sub>4</sub>	0.33	Covalent	1.057
104	Ge <sub>3</sub> H <sub>11</sub>	0.33	Covalent	1.281
105	GeH <sub>3</sub>	0.31	Covalent	1.360
106	GeH <sub>3</sub>	0.32	Covalent	1.553
107	SnH <sub>8</sub>	0.24	Molecular	0.860
108	SnH <sub>4</sub>	0.22	Molecular	0.792
109	SnH <sub>4</sub>	0.24	Molecular	0.816
110	SnH <sub>4</sub>	-	-	-
111	SnH <sub>4</sub>	0.29	Molecular	0.807
112	SnH <sub>4</sub>	-	-	-
113	SnH <sub>12</sub>	0.34	Molecular	0.754
114	SnH <sub>14</sub>	0.37	Molecular	0.783
115	PbH <sub>4</sub> (H <sub>2</sub> ) <sub>2</sub>	0.28	Molecular	0.785
116	PH <sub>3</sub>	-	-	-
117	PH	-	-	-
118	PH <sub>2</sub>	-	-	-
119	PH <sub>4</sub>	0.19	Molecular	0.740
120	PH <sub>2</sub>	0.15	Molecular	0.741
121	AsH	0.45	Covalent	1.580

122	AsH <sub>8</sub>	0.39	Molecular	0.813
123	SbH	0.35	Covalent	1.905
124	SbH <sub>3</sub>	0.27	Weak H Interactions	0.882
125	SbH <sub>4</sub>	0.29	Molecular	0.842
126	BiH <sub>2</sub>	0.32	Molecular	0.805
127	BiH <sub>3</sub>	0.31	Weak H Interactions	0.924
128	SbH <sub>3</sub>	0.35	Molecular	0.878
129	BiH	0.29	Isolated	3.033
130	BiH <sub>2</sub>	0.31	Molecular	0.812
131	BiH <sub>4</sub>	0.29	Molecular	0.834
132	BiH <sub>5</sub>	-	-	-
133	BiH <sub>6</sub>	0.37	Molecular	0.905
134	H <sub>2</sub> S	-	-	-
135	H <sub>2</sub> S	-	-	-
136	(H <sub>2</sub> S)2H <sub>2</sub>	0.69	Covalent	1.493
137	(H <sub>2</sub> S)2H <sub>2</sub>	-	-	-
138	H <sub>3</sub> S	0.7	Covalent	1.532
139	H <sub>3</sub> S	-	-	-
140	H <sub>4</sub> S <sub>3</sub>	0.44	Covalent	1.554
141	H <sub>5</sub> S <sub>2</sub>	0.56	Covalent	1.543
142	D <sub>3</sub> S	-	-	-
143	H <sub>3</sub> S <sub>0.925</sub> P <sub>0.075</sub>	-	-	-
144	H <sub>3</sub> S <sub>0.9</sub> P <sub>0.1</sub>	-	-	-
145	H <sub>3</sub> S <sub>0.96</sub> Si <sub>0.04</sub>	-	-	-
146	HSe <sub>2</sub>	0.44	Covalent	1.762
147	HSe	0.52	Covalent	2.133
148	H <sub>3</sub> Se	0.53	Covalent	1.571
149	HSe	0.52	Covalent	1.277
150	H <sub>4</sub> Te	0.4	Molecular	0.844
151	H <sub>5</sub> Te <sub>2</sub>	0.41	Weak H Interactions	0.916
152	HTe	0.41	Covalent	2.465
153	H <sub>4</sub> Te	0.35	Molecular	0.832
154	HTe	0.37	Molecular	0.834
155	PoH <sub>4</sub>	0.34	Molecular	0.813
156	PoH	0.34	Ionic	2.335
157	PoH <sub>2</sub>	0.35	Molecular	0.792
158	PoH <sub>6</sub>	0.36	Molecular	0.797
159	HBr	0.37	Covalent	1.411
160	HCl	0.37	Covalent	1.266
161	HBr	0.38	Covalent	1.492
162	HCl	0.38	Covalent	1.403
163	H <sub>2</sub> I	0.36	Molecular	0.792
164	H <sub>4</sub> I	0.45	Molecular	0.799
165	H <sub>2</sub> I	0.36	Molecular	0.797
166	H <sub>2</sub> I	0.35	Molecular	0.797
167	XeH	-	-	-
168	XeH <sub>2</sub>	-	-	-
169	MgH <sub>2</sub>	0.33	Ionic	1.763
170	MgH <sub>4</sub>	0.26	Molecular	0.776
171	MgH <sub>12</sub>	0.36	Molecular	0.819
172	PH <sub>3</sub>	-	-	-
173	PH <sub>2</sub>	0.32	Covalent	1.491
174	H <sub>2</sub> Br	-	-	-
175	H <sub>4</sub> Br	-	-	-
176	H	0.64	Weak H Interactions	0.985
177	H	0.35	Molecular	0.779

**Supplementary Data Table III:** Table reporting the item index, chemical formula, total DOS per electron, hydrogen contribution to the DOS per hydrogen atom, and hydrogen fraction of the DOS at the Fermi energy. The empty cells refer to missing values from the literature or to the impossibility to perform calculations.

Item	Chemical formula	Total DOS ( $eV^{-1}$ )	Hydrogen DOS ( $eV^{-1}$ )	Hydrogen DOS fraction
0	LiH <sub>2</sub>	0.00298	0.00709	0.94924
1	LiH <sub>2</sub>	0.02220	0.02933	0.88063
2	LiH <sub>8</sub>	0.03063	0.039	0.92588
3	KH <sub>6</sub>	0.05004	0.1429	0.87854
4	BeH <sub>2</sub>	0.01675	0.02111	0.42005
5	BeH <sub>2</sub>	0.01743	0.02091	0.39974
6	MgH <sub>6</sub>	0.02064	0.0408	0.74105
7	CaH <sub>6</sub>	0.01872	0.0456	0.91338
8	SrH <sub>6</sub>	0.01656	0.038	0.86045
9	BaH <sub>2</sub>	-	-	-
10	BaH <sub>6</sub>	-	-	-
11	ScH <sub>3</sub>	-	-	-
12	LaH <sub>3</sub>	-	-	-
13	YH <sub>3</sub>	-	-	-
14	ScH <sub>2</sub>	0.03600	0.00638	0.02726
15	YH <sub>4</sub>	0.03105	0.04555	0.39112
16	YH <sub>6</sub>	0.04132	0.053	0.45269
17	ScH <sub>4</sub>	0.03179	0.0356	0.29856
18	ScH <sub>6</sub>	0.03896	0.0356	0.32246
19	PrH <sub>9</sub>	0.01967	0.01129	0.16150
20	CeH <sub>10</sub>	0.01466	0.01309	0.27900
21	CeH <sub>9</sub>	0.02029	0.02036	0.29135
22	LaH <sub>9</sub>	0.03072	0.01651	0.16123
23	LaH <sub>6</sub>	-	-	-
24	YH <sub>9</sub>	0.02762	0.04033	0.65701
25	ScH <sub>9</sub>	0.02564	0.03135	0.55013
27	YH <sub>10</sub>	0.03547	0.04992	0.67017
28	LaH <sub>4</sub>	-	-	-
29	LaH <sub>8</sub>	0.01605	0.02265	0.38922
30	LaH <sub>10</sub>	0.02601	0.04064	0.50395
31	ScH <sub>9</sub>	0.02952	0.03491	0.53215
32	ScH <sub>10</sub>	0.02176	0.02453	0.53668
33	ScH <sub>12</sub>	0.02376	0.02673	0.58697
34	ScH <sub>7</sub>	0.02505	0.03605	0.55962
35	ScH <sub>3</sub>	-	-	-
36	ScH <sub>2</sub>	-	-	-
37	ScH <sub>6</sub>	0.02758	0.0336	0.42992
38	TiD <sub>0.74</sub>	-	-	-
39	TiH <sub>2</sub>	0.17927	0.00066	0.00053
40	TiH <sub>2</sub>	0.05533	0.01472	0.03800
41	ZrH	0.07636	0.01206	0.01214
42	HfH <sub>2</sub>	0.01242	0.00186	0.00787
43	HfH <sub>2</sub>	0.01072	0.02352	0.11542
44	HfH <sub>2</sub>	0.00907	0.01225	0.07105
45	NbH <sub>2</sub>	0.03424	0.00216	0.00844
46	VH <sub>2</sub>	0.08699	0.00352	0.00539
47	NbH <sub>2</sub>	0.06102	0.00306	0.00668
48	NbH <sub>2</sub>	0.06066	0.00522	0.01147
49	NbH <sub>4</sub>	0.04581	0.021	0.10784
50	TaH <sub>2</sub>	0.02064	0.0091	0.03040
51	TaH <sub>4</sub>	0.01307	0.02355	0.23240
52	TaH <sub>6</sub>	0.01519	0.0403	0.48226
53	CrH	0.06706	0.0064	0.00636
54	CrH <sub>3</sub>	0.07060	0.0282	0.07048
55	TcH <sub>2</sub>	-	-	-
56	TcH <sub>2</sub>	-	-	-
57	TcH <sub>3</sub>	0.03144	0.0138	0.07314

58	FeH <sub>6</sub>	0.02460	0.01662	0.18419
59	FeH <sub>5</sub>	0.02408	0.00616	0.06091
60	FeH <sub>5</sub>	-	-	-
61	RuH	0.04832	0.0133	0.01618
62	RuH <sub>3</sub>	0.04596	0.024	0.08244
63	RuH <sub>3</sub>	0.02571	0.022	0.13508
64	OsH	0.02037	0.00498	0.00788
65	CoH	0.24733	0.02135	0.00479
66	R <sub>H</sub> H	-	-	-
67	IrH	-	-	-
68	PdH	0.02481	0.0745	0.15803
69	PdD	-	-	-
70	PdH	0.02481	0.0745	0.15803
71	PdD	-	-	-
72	PdT	-	-	-
73	PtH	0.01163	0.0562	0.14640
74	PtH	0.01735	0.047	0.08208
75	AuH	0.02019	0.01531	0.02230
76	BH	0.02755	0.03	0.27223
77	BH <sub>3</sub>	0.02614	0.028	0.53550
78	AlH <sub>3</sub>	0.03379	0.0458	0.67764
79	AlH <sub>3</sub> (H <sub>2</sub> )	-	-	-
80	GaH <sub>3</sub>	0.01841	0.0208	0.56491
81	InH <sub>5</sub>	0.02133	0.02644	0.34432
82	InH <sub>3</sub>	0.02221	0.03366	0.28419
83	SiH <sub>4</sub>	0.03007	0.0359	0.59684
84	SiH <sub>4</sub>	0.05725	0.0464	0.40524
85	SiH <sub>4</sub>	-	-	-
86	SiH <sub>4</sub>	-	-	-
87	SiH <sub>4</sub>	0.02126	0.02338	0.54972
88	SiH <sub>4</sub>	0.03087	0.02732	0.44245
89	SiH <sub>4</sub>	0.03394	0.01705	0.25117
90	SiH <sub>4</sub>	-	-	-
91	SiH <sub>4</sub>	0.0195	0.0243	0.62307
92	SiH <sub>4</sub> H <sub>2</sub>	-	-	-
93	Si <sub>2</sub> H <sub>6</sub>	0.03554	0.0297	0.35811
94	Si <sub>2</sub> H <sub>6</sub>	0.04522	0.0392	0.37144
95	Si <sub>2</sub> H <sub>6</sub>	0.04734	0.03976	0.35998
96	Si <sub>2</sub> H <sub>6</sub>	-	-	-
97	GeH <sub>4</sub>	0.01901	0.0314	0.36688
98	GeH <sub>4</sub>	-	-	-
99	GeH <sub>4</sub>	0.01805	0.03362	0.41384
100	GeH <sub>4</sub>	0.01439	0.03255	0.50236
101	GeH <sub>4</sub> (H <sub>2</sub> ) <sub>2</sub>	0.01920	0.0279	0.52831
102	GeH <sub>3</sub>	-	-	-
103	GeH <sub>4</sub>	0.01449	0.02803	0.42974
104	Ge <sub>3</sub> H <sub>11</sub>	0.01079	0.02473	0.47560
105	GeH <sub>3</sub>	0.02187	0.03453	0.27853
106	GeH <sub>3</sub>	0.03444	0.0484	0.24793
107	SnH <sub>8</sub>	0.01736	0.02607	0.54617
108	SnH <sub>4</sub>	0.01782	0.0241	0.30038
109	SnH <sub>4</sub>	0.0223	0.0372	0.37070
110	SnH <sub>4</sub>	-	-	-
111	SnH <sub>4</sub>	0.01920	0.0331	0.38303
112	SnH <sub>4</sub>	-	-	-
113	SnH <sub>12</sub>	0.02066	0.02871	0.64144
114	SnH <sub>14</sub>	0.02083	0.02999	0.71983
115	PbH <sub>4</sub> (H <sub>2</sub> ) <sub>2</sub>	0.02688	0.03232	0.43717
116	PH <sub>3</sub>	-	-	-
117	PH	-	-	-
118	PH <sub>2</sub>	-	-	-
119	PH <sub>4</sub>	0.02710	0.01734	0.28436
120	PH <sub>2</sub>	0.03010	0.01784	0.16935
121	AsH	0.01920	0.052	0.16926

122	AsH <sub>8</sub>	0.02111	0.03243	0.53430
123	SbH	0.02155	0.0482	0.13976
124	SbH <sub>3</sub>	0.01877	0.037	0.62715
125	SbH <sub>4</sub>	0.03026	0.0465	0.32348
126	BiH <sub>2</sub>	0.02709	0.0446	0.19364
127	BiH <sub>3</sub>	0.02584	0.0537	0.34636
128	SbH <sub>3</sub>	0.02447	0.0408	0.27787
129	BiH	0.02447	0.09	0.22987
130	BiH <sub>2</sub>	0.02626	0.0485	0.21725
131	BiH <sub>4</sub>	0.02858	0.0402	0.29603
132	BiH <sub>5</sub>	-	-	-
133	BiH <sub>6</sub>	0.02549	0.04146	0.46471
134	H <sub>2</sub> S	-	-	-
135	H <sub>2</sub> S	-	-	-
136	(H <sub>2</sub> S)2H <sub>2</sub>	0.06064	0.0867	0.47654
137	(H <sub>2</sub> S)2H <sub>2</sub>	-	-	-
138	H <sub>3</sub> S	0.05348	0.0782	0.48732
139	H <sub>3</sub> S	-	-	-
140	H <sub>4</sub> S <sub>3</sub>	0.01120	0.01403	0.22762
141	H <sub>5</sub> S <sub>2</sub>	0.03182	0.0442	0.40847
142	D <sub>3</sub> S	-	-	-
143	H <sub>3</sub> S <sub>0.925</sub> P <sub>0.075</sub>	-	-	-
144	H <sub>3</sub> S <sub>0.9</sub> P <sub>0.1</sub>	-	-	-
145	H <sub>3</sub> S <sub>0.96</sub> Si <sub>0.04</sub>	-	-	-
146	HSe <sub>2</sub>	0.01736	0.0819	0.14294
147	HSe	0.02240	0.0544	0.14283
148	H <sub>3</sub> Se	0.02796	0.0857	0.48394
149	HSe	0.01874	0.0494	0.15501
150	H <sub>4</sub> Te	0.03724	0.0464	0.24914
151	H <sub>5</sub> Te <sub>2</sub>	0.02416	0.04592	0.25675
152	HTe	0.02680	0.065	0.14264
153	H <sub>4</sub> Te	0.02674	0.0381	0.28495
154	HTe	0.03070	0.0424	0.27614
155	PoH <sub>4</sub>	0.02522	0.0359	0.28468
156	PoH	0.02491	0.0864	0.20401
157	PoH <sub>2</sub>	0.02682	0.0405	0.16772
158	PoH <sub>6</sub>	0.03239	0.03846	0.32384
159	HBr	0.01632	0.052	0.17697
160	HCl	0.01352	0.0432	0.17748
161	HBr	0.01836	0.0454	0.13735
162	HCl	0.03575	0.0388	0.13565
163	H <sub>2</sub> I	0.02955	0.0269	0.09580
164	H <sub>4</sub> I	0.01606	0.0262	0.31063
165	H <sub>2</sub> I	0.02681	0.0298	0.11697
166	H <sub>2</sub> I	0.02684	0.042	0.16466
167	XeH	-	-	-
168	XeH <sub>2</sub>	-	-	-
169	MgH <sub>2</sub>	0.00801	0.01701	0.35378
170	MgH <sub>4</sub>	0.00576	0.01346	0.66683
171	MgH <sub>12</sub>	0.01311	0.0221	0.91945
172	PH <sub>3</sub>	-	-	-
173	PH <sub>2</sub>	0.04305	0.061	0.40477
174	H <sub>2</sub> Br	-	-	-
175	H <sub>4</sub> Br	-	-	-
176	H	0.03300	0.033	1
177	H	0.01878	0.01878	1

---

[1] Yu Xie, Quan Li, Artem R. Oganov, and Hui Wang. Superconductivity of lithium-doped hydrogen under high pressure. *Acta Crystallographica Section C*, 70(2):104–111, Feb 2014.



- [2] Dawei Zhou, Xilian Jin, Xing Meng, Gang Bao, Yanming Ma, Bingbing Liu, and Tian Cui. Ab initio study revealing a layered structure in hydrogen-rich  $\text{Kh}_6$  under high pressure. *Phys. Rev. B*, 86:014118, Jul 2012.
- [3] Shuyin Yu, Qingfeng Zeng, Artem R. Oganov, Chaohao Hu, Gilles Frapper, and Litong Zhang. Exploration of stable compounds, crystal structures, and superconductivity in the be-h system. *AIP Advances*, 4(10):107118, 2014.
- [4] Xiaolei Feng, Jurong Zhang, Guoying Gao, Hanyu Liu, and Hui Wang. Compressed sodalite-like  $\text{mgH}_6$  as a potential high-temperature superconductor. *RSC Adv.*, 5:59292–59296, 2015.
- [5] Hui Wang, John S. Tse, Kaori Tanaka, Toshiaki Iitaka, and Yanming Ma. Superconductive sodalite-like clathrate calcium hydride at high pressures. *Proceedings of the National Academy of Sciences*, 109(17):6463–6466, 2012.
- [6] Yanchao Wang, Hui Wang, John S. Tse, Toshiaki Iitaka, and Yanming Ma. Structural morphologies of high-pressure polymorphs of strontium hydrides. *Phys. Chem. Chem. Phys.*, 17:19379–19385, 2015.
- [7] James Hooper, Bahadır Altintas, Andrew Shamp, and Eva Zurek. Polyhydrides of the alkaline earth metals: A look at the extremes under pressure. *The Journal of Physical Chemistry C*, 117(6):2982–2992, 2013.
- [8] Duck Young Kim, Ralph H. Scheicher, Ho-kwang Mao, Tae W. Kang, and Rajeev Ahuja. General trend for pressurized superconducting hydrogen-dense materials. *Proceedings of the National Academy of Sciences*, 107(7):2793–2796, 2010.
- [9] Yong-Kai Wei, Jiao-Nan Yuan, Faez Iqbal Khan, Guang-Fu Ji, Zhuo-Wei Gu, and Dong-Qing Wei. Pressure induced superconductivity and electronic structure properties of scandium hydrides using first principles calculations. *RSC Adv.*, 6:81534–81541, 2016.
- [10] Yinwei Li, Jian Hao, Hanyu Liu, S Tse John, Yanchao Wang, and Yanming Ma. Pressure-stabilized superconductive yttrium hydrides. *Scientific Reports*, 5:9948, 2015.
- [11] Shifeng Qian, Xiaowei Sheng, Xiaozhen Yan, Yangmei Chen, and Bo Song. Theoretical study of stability and superconductivity of  $\text{sch}_n$  ( $n = 4 - 8$ ) at high pressure. *Phys. Rev. B*, 96:094513, Sep 2017.
- [12] Xiaoqiu Ye, Nilofar Zarifi, Eva Zurek, Roald Hoffmann, and NW Ashcroft. High hydrides of scandium under pressure: potential superconductors. *The Journal of Physical Chemistry C*, 122(11):6298–6309, 2018.
- [13] Feng Peng, Ying Sun, Chris J. Pickard, Richard J. Needs, Qiang Wu, and Yanming Ma. Hydrogen clathrate structures in rare earth hydrides at high pressures: Possible route to room-temperature superconductivity. *Phys. Rev. Lett.*, 119:107001, Sep 2017.
- [14] Bin Li, Zilong Miao, Lei Ti, Shengli Liu, Jie Chen, Zhixiang Shi, and Eugene Gregoryanz. Predicted high-temperature superconductivity in cerium hydrides at high pressures. *Journal of Applied Physics*, 126(23):235901, 2019.
- [15] Hanyu Liu, Ivan I. Naumov, Roald Hoffmann, N. W. Ashcroft, and Russell J. Hemley. Potential high- $T_c$  superconducting lanthanum and yttrium hydrides at high pressure. *Proceedings of the National Academy of Sciences*, 114(27):6990–6995, 2017.
- [16] IO Bashkin, MV Nefedova, VG Tissen, and EG Ponyatovskii. Superconductivity in the ti-d system under pressure. *Physics of the Solid State*, 40(12):1950–1952, 1998.
- [17] Kavungal Veedu Shanavas, L Lindsay, and David S Parker. Electronic structure and electron-phonon coupling in  $\text{tih}_2$ . *Scientific Reports*, 6:28102, 2016.
- [18] Xiao-Feng Li, Zi-Yu Hu, and Bing Huang. Phase diagram and superconductivity of compressed zirconium hydrides. *Phys. Chem. Chem. Phys.*, 19:3538–3543, 2017.
- [19] Yunxian Liu, Xiaoli Huang, Defang Duan, Fubo Tian, Hanyu Liu, Da Li, Zhonglong Zhao, Xiaojing Sha, Hongyu Yu, Huadi Zhang, et al. First-principles study on the structural and electronic properties of metallic  $\text{hfh}_2$  under pressure. *Scientific reports*, 5:11381, 2015.
- [20] Changbo Chen, Fubo Tian, Defang Duan, Kuo Bao, Xilian Jin, Bingbing Liu, and Tian Cui. Pressure induced phase transition in  $\text{mh}_2$  ( $m = \text{v}, \text{nb}$ ). *The Journal of Chemical Physics*, 140(11):114703, 2014.
- [21] Guoying Gao, Roald Hoffmann, N. W. Ashcroft, Hanyu Liu, Aitor Bergara, and Yanming Ma. Theoretical study of the ground-state structures and properties of niobium hydrides under pressure. *Phys. Rev. B*, 88:184104, Nov 2013.
- [22] Quan Zhuang, Xilian Jin, Tian Cui, Yanbin Ma, Qianqian Lv, Ying Li, Huadi Zhang, Xing Meng, and Kuo Bao. Pressure-stabilized superconductive ionic tantalum hydrides. *Inorganic chemistry*, 56(7):3901–3908, 2017.
- [23] Shuyin Yu, Xiaojing Jia, Gilles Frapper, Duan Li, Artem R Oganov, Qingfeng Zeng, and Litong Zhang. Pressure-driven formation and stabilization of superconductive chromium hydrides. *Scientific reports*, 5:17764, 2015.
- [24] Xiaofeng Li, Hanyu Liu, and Feng Peng. Crystal structures and superconductivity of technetium hydrides under pressure. *Phys. Chem. Chem. Phys.*, 18:28791–28796, 2016.
- [25] Alexander G Kvashnin, Ivan A Kruglov, Dmitrii V Semenok, and Artem R Oganov. Iron superhydrides  $\text{feh}_5$  and  $\text{feh}_6$ : stability, electronic properties, and superconductivity. *The Journal of Physical Chemistry C*, 122(8):4731–4736, 2018.
- [26] Arnab Majumdar, John S. Tse, Min Wu, and Yansun Yao. Superconductivity in  $\text{feh}_5$ . *Phys. Rev. B*, 96:201107, Nov 2017.
- [27] Yunxian Liu, Defang Duan, Fubo Tian, Chao Wang, Yanbin Ma, Da Li, Xiaoli Huang, Bingbing Liu, and Tian Cui. Stability and properties of the  $\text{ru-h}$  system at high pressure. *Phys. Chem. Chem. Phys.*, 18:1516–1520, 2016.
- [28] Yunxian Liu, Defang Duan, Xiaoli Huang, Fubo Tian, Da Li, Xiaojing Sha, Chao Wang, Huadi Zhang, Ting Yang, Bingbing Liu, et al. Structures and properties of osmium hydrides under pressure from first principle calculation. *The Journal of Physical Chemistry C*, 119(28):15905–15911, 2015.
- [29] Liyuan Wang, Defang Duan, Hongyu Yu, Hui Xie, Xiaoli Huang, Yanbin Ma, Fubo Tian, Da Li, Bingbing Liu, and Tian Cui. High-pressure formation of cobalt polyhydrides: A first-principle study. *Inorganic Chemistry*, 57(1):181–186, 2018.
- [30] Tiange Bi, Nilofar Zarifi, Tyson Terpstra, and Eva Zurek. The search for superconductivity in high pressure hydrides. In *Reference Module in Chemistry, Molecular Sciences and Chemical Engineering*. Elsevier, 2019.
- [31] B Stritzker and W Buckel. Superconductivity in the palladium-hydrogen and the palladium-deuterium systems. *Zeitschrift für Physik A Hadrons and nuclei*, 257(1):1–8, 1972.

- [32] Ion Errea, Matteo Calandra, and Francesco Mauri. First-principles theory of anharmonicity and the inverse isotope effect in superconducting palladium-hydride compounds. *Physical review letters*, 111(17):177002, 2013.
- [33] Chao-Hao Hu, Artem R Oganov, Qiang Zhu, Guang-Rui Qian, Gilles Frapper, Andriy O Lyakhov, and Huai-Ying Zhou. Pressure-induced stabilization and insulator-superconductor transition of bh. *Physical review letters*, 110(16):165504, 2013.
- [34] Kazutaka Abe and NW Ashcroft. Crystalline diborane at high pressures. *Physical Review B*, 84(10):104118, 2011.
- [35] Yong-Kai Wei, Ni-Na Ge, Guang-Fu Ji, Xiang-Rong Chen, Ling-Cang Cai, Su-Qin Zhou, and Dong-Qing Wei. Elastic, superconducting, and thermodynamic properties of the cubic metallic phase of alh<sub>3</sub> via first-principles calculations. *Journal of Applied Physics*, 114(11):114905, 2013.
- [36] Igor Goncharenko, MI Eremets, M Hanfland, JS Tse, M Amboage, Y Yao, and IA Trojan. Pressure-induced hydrogen-dominant metallic state in aluminum hydride. *Physical Review Letters*, 100(4):045504, 2008.
- [37] Pugeng Hou, Xiusong Zhao, Fubo Tian, Da Li, Defang Duan, Zhonglong Zhao, Binhua Chu, Bingbing Liu, and Tian Cui. High pressure structures and superconductivity of alh<sub>3</sub>(h<sub>2</sub>) predicted by first principles. *RSC Adv.*, 5:5096–5101, 2015.
- [38] Guoying Gao, Hui Wang, Aitor Bergara, Yinwei Li, Guangtao Liu, and Yanming Ma. Metallic and superconducting gallane under high pressure. *Physical Review B*, 84(6):064118, 2011.
- [39] Yunxian Liu, Defang Duan, Fubo Tian, Hanyu Liu, Chao Wang, Xiaoli Huang, Da Li, Yanbin Ma, Bingbing Liu, and Tian Cui. Pressure-induced structures and properties in indium hydrides. *Inorganic chemistry*, 54(20):9924–9928, 2015.
- [40] Y Yao, J. S Tse, Y Ma, and K Tanaka. Superconductivity in high-pressure SiH<sub>4</sub>. *Europhysics Letters (EPL)*, 78(3):37003, apr 2007.
- [41] JS Tse, Y Yao, and K Tanaka. Novel superconductivity in metallic snh<sub>4</sub> under high pressure. *Physical Review Letters*, 98(11):117004, 2007.
- [42] Ji Feng, Wojciech Grochala, Tomasz Jaroń, Roald Hoffmann, Aitor Bergara, and NW Ashcroft. Structures and potential superconductivity in sih<sub>4</sub> at high pressure: En route to "metallic hydrogen". *Physical Review Letters*, 96(1):017006, 2006.
- [43] Huadi Zhang, Xilian Jin, Yunzhou Lv, Quan Zhuang, Yunxian Liu, Qianqian Lv, Kuo Bao, Da Li, Bingbing Liu, and Tian Cui. High-temperature superconductivity in compressed solid silane. *Scientific reports*, 5:8845, 2015.
- [44] Xiao-Jia Chen, Jiang-Long Wang, Viktor V Struzhkin, Ho-kwang Mao, Russell J Hemley, and Hai-Qing Lin. Superconducting behavior in compressed solid sih<sub>4</sub> with a layered structure. *Physical review letters*, 101(7):077002, 2008.
- [45] Miguel Martinez-Canales, Artem R Oganov, Yanming Ma, Yan Yan, Andriy O Lyakhov, and Aitor Bergara. Novel structures and superconductivity of silane under pressure. *Physical review letters*, 102(8):087005, 2009.
- [46] Yinwei Li, Guoying Gao, Yu Xie, Yanming Ma, Tian Cui, and Guangtian Zou. Superconductivity at 100 k in dense sih<sub>4</sub> (h<sub>2</sub>)<sub>2</sub> predicted by first principles. *Proceedings of the National Academy of Sciences*, 107(36):15708–15711, 2010.
- [47] Xilian Jin, Xing Meng, Zhi He, Yanming Ma, Bingbing Liu, Tian Cui, Guangtian Zou, and Ho-kwang Mao. Superconducting high-pressure phases of disilane. *Proceedings of the National Academy of Sciences*, 107(22):9969–9973, 2010.
- [48] Guoying Gao, Artem R Oganov, Aitor Bergara, Miguel Martinez-Canales, Tian Cui, Toshiaki Iitaka, Yanming Ma, and Guangtian Zou. Superconducting high pressure phase of germane. *Physical review letters*, 101(10):107002, 2008.
- [49] Chao Zhang, Xiao-Jia Chen, Yan-Ling Li, Viktor V Struzhkin, Russell J Hemley, Ho-Kwang Mao, Rui-Qin Zhang, and Hai-Qing Lin. Superconductivity in hydrogen-rich material: Geh<sub>4</sub>. *Journal of superconductivity and novel magnetism*, 23(5):717–719, 2010.
- [50] Huadi Zhang, Xilian Jin, Yunzhou Lv, Quan Zhuang, Qianqian Lv, Yunxian Liu, Kuo Bao, Da Li, Bingbing Liu, and Tian Cui. Investigation of stable germane structures under high-pressure. *Physical Chemistry Chemical Physics*, 17(41):27630–27635, 2015.
- [51] Guohua Zhong, Chao Zhang, Xiaojia Chen, Yanling Li, Ruiqin Zhang, and Haiqing Lin. Structural, electronic, dynamical, and superconducting properties in dense geh<sub>4</sub> (h<sub>2</sub>)<sub>2</sub>. *The Journal of Physical Chemistry C*, 116(8):5225–5234, 2012.
- [52] PuGeng Hou, FuBo Tian, Da Li, ZhongLong Zhao, DeFang Duan, HuaDi Zhang, XiaoJing Sha, BingBing Liu, and Tian Cui. Ab initio study of germanium-hydride compounds under high pressure. *RSC advances*, 5(25):19432–19438, 2015.
- [53] M Mahdi Davari Esfahani, Artem R Oganov, Haiyang Niu, and Jin Zhang. Superconductivity and unexpected chemistry of germanium hydrides under pressure. *Physical Review B*, 95(13):134506, 2017.
- [54] Kazutaka Abe and NW Ashcroft. Quantum disproportionation: The high hydrides at elevated pressures. *Physical Review B*, 88(17):174110, 2013.
- [55] Huadi Zhang, Xilian Jin, Yunzhou Lv, Quan Zhuang, Yunxian Liu, Qianqian Lv, Da Li, Kuo Bao, Bingbing Liu, and Tian Cui. A novel stable hydrogen-rich snh<sub>8</sub> under high pressure. *RSC advances*, 5(130):107637–107641, 2015.
- [56] Guoying Gao, Artem R Oganov, Peifang Li, Zhenwei Li, Hui Wang, Tian Cui, Yanming Ma, Aitor Bergara, Andriy O Lyakhov, Toshiaki Iitaka, et al. High-pressure crystal structures and superconductivity of stannane (snh<sub>4</sub>). *Proceedings of the National Academy of Sciences*, 107(4):1317–1320, 2010.
- [57] JS Tse, Y Yao, and K Tanaka. Novel superconductivity in metallic snh<sub>4</sub> under high pressure. *Physical Review Letters*, 98(11):117004, 2007.
- [58] Huadi Zhang, Xilian Jin, Yunzhou Lv, Quan Zhuang, Ying Li, Kuo Bao, Da Li, Bingbing Liu, and Tian Cui. Pressure-induced phase transition of snh<sub>4</sub>: a new layered structure. *RSC Adv.*, 6:10456–10461, 2016.
- [59] M Mahdi Davari Esfahani, Zhenhai Wang, Artem R Oganov, Huafeng Dong, Qiang Zhu, Shengnan Wang, Maksim S Rakitin, and Xiang-Feng Zhou. Superconductivity of novel tin hydrides (sn n h m) under pressure. *Scientific reports*, 6:22873, 2016.
- [60] I. A. Troyan A.P. Drozdov, M. I. Eremets. Superconductivity above 100 k in ph<sub>3</sub> at high pressures. *arXiv:1508.06224*.
- [61] José A Flores-Livas, Maximilian Amsler, Christoph Heil, Antonio Sanna, Lilia Boeri, Gianni Profeta, Chris Wolverton, Stefan Goedecker, and EKV Gross. Superconductivity in metastable phases of phosphorus-hydride compounds under high pressure. *Physical Review B*, 93(2):020508, 2016.
- [62] Hanyu Liu, Yinwei Li, Guoying Gao, John S Tse, and Ivan I Naumov. Crystal structure and superconductivity of ph<sub>3</sub> at

- high pressures. *The Journal of Physical Chemistry C*, 120(6):3458–3461, 2016.
- [63] Tiange Bi, Daniel P Miller, Andrew Shamp, and Eva Zurek. Superconducting phases of phosphorus hydride under pressure: stabilization by mobile molecular hydrogen. *Angewandte Chemie*, 129(34):10326–10329, 2017.
  - [64] Tiange Bi, Daniel P Miller, Andrew Shamp, and Eva Zurek. Superconducting phases of phosphorus hydride under pressure: stabilization by mobile molecular hydrogen. *Angewandte Chemie*, 129(34):10326–10329, 2017.
  - [65] Yuhao Fu, Xiangpo Du, Lijun Zhang, Feng Peng, Miao Zhang, Chris J Pickard, Richard J Needs, David J Singh, Weitao Zheng, and Yanming Ma. High-pressure phase stability and superconductivity of pnictogen hydrides and chemical trends for compressed hydrides. *Chemistry of Materials*, 28(6):1746–1755, 2016.
  - [66] Kazutaka Abe and NW Ashcroft. Stabilization and highly metallic properties of heavy group-v hydrides at high pressures. *Physical Review B*, 92(22):224109, 2015.
  - [67] Yanbin Ma, Defang Duan, Da Li, Yunxian Liu, Fubo Tian, Hongyu Yu, Chunhong Xu, Ziji Shao, Bingbing Liu, and Tian Cui. High-pressure structures and superconductivity of bismuth hydrides. *arXiv preprint arXiv:1511.05291*, 2015.
  - [68] Yinwei Li, Jian Hao, Hanyu Liu, Yanling Li, and Yanming Ma. The metallization and superconductivity of dense hydrogen sulfide. *The Journal of chemical physics*, 140(17):174712, 2014.
  - [69] Defang Duan, Yunxian Liu, Fubo Tian, Da Li, Xiaoli Huang, Zhonglong Zhao, Hongyu Yu, Bingbing Liu, Wenjing Tian, and Tian Cui. Pressure-induced metallization of dense (h 2 s) 2 h 2 with high-t c superconductivity. *Scientific reports*, 4:6968, 2014.
  - [70] Ion Errea, Matteo Calandra, Chris J Pickard, Joseph R Nelson, Richard J Needs, Yinwei Li, Hanyu Liu, Yunwei Zhang, Yanming Ma, and Francesco Mauri. Quantum hydrogen-bond symmetrization in the superconducting hydrogen sulfide system. *Nature*, 532(7597):81–84, 2016.
  - [71] Ryosuke Akashi, Mitsunori Kawamura, Shinji Tsuneyuki, Yusuke Nomura, and Ryotaro Arita. First-principles study of the pressure and crystal-structure dependences of the superconducting transition temperature in compressed sulfur hydrides. *Physical Review B*, 91(22):224513, 2015.
  - [72] Yinwei Li, Lin Wang, Hanyu Liu, Yunwei Zhang, Jian Hao, Chris J Pickard, Joseph R Nelson, Richard J Needs, Wentao Li, Yanwei Huang, et al. Dissociation products and structures of solid h 2 s at strong compression. *Physical Review B*, 93(2):020103, 2016.
  - [73] Takahiro Ishikawa, Akitaka Nakanishi, Katsuya Shimizu, Hiroshi Katayama-Yoshida, Tatsuki Oda, and Naoshi Suzuki. Superconducting h 5 s 2 phase in sulfur-hydrogen system under high-pressure. *Scientific reports*, 6:23160, 2016.
  - [74] José A Flores-Livas, Antonio Sanna, and EKH Gross. High temperature superconductivity in sulfur and selenium hydrides at high pressure. *The European Physical Journal B*, 89(3):63, 2016.
  - [75] Yanfeng Ge, Fan Zhang, and Yugui Yao. First-principles demonstration of superconductivity at 280 k in hydrogen sulfide with low phosphorus substitution. *Physical Review B*, 93(22):224513, 2016.
  - [76] Shoutao Zhang, Yanchao Wang, Jurong Zhang, Hanyu Liu, Xin Zhong, Hai-Feng Song, Guochun Yang, Lijun Zhang, and Yanming Ma. Phase diagram and high-temperature superconductivity of compressed selenium hydrides. *Scientific reports*, 5(1):1–8, 2015.
  - [77] Xin Zhong, Hui Wang, Jurong Zhang, Hanyu Liu, Shoutao Zhang, Hai-Feng Song, Guochun Yang, Lijun Zhang, and Yanming Ma. Tellurium hydrides at high pressures: High-temperature superconductors. *Physical Review Letters*, 116(5):057002, 2016.
  - [78] Yunxian Liu, Defang Duan, Fubo Tian, Chao Wang, Gang Wu, Yanbin Ma, Hongyu Yu, Da Li, Bingbing Liu, and Tian Cui. Prediction of stoichiometric poh n compounds: crystal structures and properties. *RSC advances*, 5(125):103445–103450, 2015.
  - [79] Defang Duan, Fubo Tian, Zhi He, Xing Meng, Liancheng Wang, Changbo Chen, Xiusong Zhao, Bingbing Liu, and Tian Cui. Hydrogen bond symmetrization and superconducting phase of hbr and hcl under high pressure: An ab initio study. *The Journal of chemical physics*, 133(7):074509, 2010.
  - [80] Defang Duan, Fubo Tian, Zhi He, Xing Meng, Liancheng Wang, Changbo Chen, Xiusong Zhao, Bingbing Liu, and Tian Cui. Hydrogen bond symmetrization and superconducting phase of hbr and hcl under high pressure: An ab initio study. *The Journal of chemical physics*, 133(7):074509, 2010.
  - [81] Siyu Lu, Min Wu, Hanyu Liu, S Tse John, and Bai Yang. Prediction of novel crystal structures and superconductivity of compressed hbr. *RSC Advances*, 5(57):45812–45816, 2015.
  - [82] Changbo Chen, Ying Xu, Xiuping Sun, and Sihan Wang. Novel superconducting phases of hcl and hbr under high pressure: an ab initio study. *The Journal of Physical Chemistry C*, 119(30):17039–17043, 2015.
  - [83] Andrew Shamp and Eva Zurek. Superconducting high-pressure phases composed of hydrogen and iodine. *The Journal of Physical Chemistry Letters*, 6(20):4067–4072, 2015.
  - [84] Defang Duan, Fubo Tian, Yunxian Liu, Xiaoli Huang, Da Li, Hongyu Yu, Yanbin Ma, Bingbing Liu, and Tian Cui. Enhancement of t c in the atomic phase of iodine-doped hydrogen at high pressures. *Physical Chemistry Chemical Physics*, 17(48):32335–32340, 2015.
  - [85] Xiaozhen Yan, Yangmei Chen, Xiaoyu Kuang, and Shikai Xiang. Structure, stability, and superconductivity of new xe–h compounds under high pressure. *The Journal of chemical physics*, 143(12):124310, 2015.
  - [86] David C Lonie, James Hooper, Bahadır Altintas, and Eva Zurek. Metallization of magnesium polyhydrides under pressure. *Physical Review B*, 87(5):054107, 2013.
  - [87] José A Flores-Livas, Maximilian Amsler, Christoph Heil, Antonio Sanna, Lilia Boeri, Gianni Profeta, Chris Wolverton, Stefan Goedecker, and EKH Gross. Superconductivity in metastable phases of phosphorus-hydride compounds under high pressure. *Physical Review B*, 93(2):020508, 2016.
  - [88] Andrew Shamp, Tyson Terpstra, Tiange Bi, Zackary Falls, Patrick Avery, and Eva Zurek. Decomposition products of phosphine under pressure: Ph2 stable and superconducting? *Journal of the American Chemical Society*, 138(6):1884–1892,

- 2016.
- [89] Defang Duan, Fubo Tian, Xiaoli Huang, Da Li, Hongyu Yu, Yunxian Liu, Yanbin Ma, Bingbing Liu, and Tian Cui. Decomposition of solid hydrogen bromide at high pressure. *arXiv preprint arXiv:1504.01196*, 2015.
  - [90] Miguel Borinaga, Ion Errea, Matteo Calandra, Francesco Mauri, and Aitor Bergara. Anharmonic effects in atomic hydrogen: Superconductivity and lattice dynamical stability. *Physical Review B*, 93(17):174308, 2016.
  - [91] Miguel Borinaga, P Riego, A Leonardo, Matteo Calandra, Francesco Mauri, Aitor Bergara, and Ion Errea. Anharmonic enhancement of superconductivity in metallic molecular cmca- 4 hydrogen at high pressure: a first-principles study. *Journal of Physics: Condensed Matter*, 28(49):494001, 2016.